

# UC Davis

## UC Davis Electronic Theses and Dissertations

### Title

Pre-Mitotic and Mitotic Events of Equine Embryo Development

### Permalink

<https://escholarship.org/uc/item/6h04t3g1>

### Author

Kato, Momoe

### Publication Date

2022

Peer reviewed|Thesis/dissertation

Pre-Mitotic and Mitotic Events of Equine Embryo Development

By

MOMOE KATO  
DISSERTATION

Submitted in partial satisfaction of the requirements for the degree of

Doctor of Philosophy

in

ANIMAL BIOLOGY

in the

OFFICE OF GRADUATE STUDIES

of the

UNIVERSITY OF CALIFORNIA

DAVIS

Approved:

---

Stuart Meyers, Chair

---

Pouya Dini

---

Shawn Chavez

Committee in Charge

2022

# TABLE OF CONTENTS

Acknowledgements.....	iii
Dissertation Abstract	iv
Chapter 1: Introduction to the dissertation.....	1
Chapter 2: Review of Relevant Literature.....	3
In vitro production in the horse ( <i>Equus ferus caballus</i> ).....	3
Early embryonic development in mammalian species.....	6
Pronuclear (PN) formation and cytoplasmic extrusion (CE) in equine embryos.....	8
Time-lapse microscopy (TLM) of preimplantation development.....	9
Meiotic errors lead to aneuploidy in oocytes and embryos.....	11
Contribution of mitotic errors to embryonic aneuploidy and mosaicism.....	14
Aneuploidy screening via embryo biopsy and non-invasive methods.....	15
Summary and conclusions.....	16
References.....	18
Chapter 3: Pronuclear formation and cytoplasmic extrusion in the early equine embryo.....	26
Introduction.....	26
Materials and Methods.....	28
Results.....	32
Discussion.....	34
Tables and Figures.....	39
References .....	47
Chapter 4: Aneuploidy in the early cleavage stage equine embryo	50
Introduction	50
Materials and Methods.....	52
Results.....	59
Discussion.....	61
Tables and Figures.....	65
References .....	70
Chapter 5: Summary and Conclusions .....	74
References .....	76

## **Acknowledgements**

I would like to thank my academic advisor, Stuart Meyers, for his guidance and mentorship throughout my graduate career. Additionally, I want to extend my gratitude to Pouya Dini for the expertise and support that he provided to complete my projects. I would also like to thank my dissertation committee members: Stuart Meyers, Pouya Dini and Shawn Chavez for their suggestions and critical feedback to improve this dissertation. It has truly been a privilege to write my dissertation under your guidance.

I am also very grateful for the support, encouragement, and teamwork I received from my colleagues and fellow lab mates Alejandro de la Fuente, Tawny Scanlan, Azarene Foutouhi, Danielle Meyers and Amie Romney through thick and thin.

Finally, I would like to express my deep and sincere gratitude to my family in the states and Japan for their love and support throughout my life. I am extremely grateful for the encouragement and moral support I received from my husband throughout my academic career.

## Dissertation Abstract

Mammalian embryo quality is often assessed by morphology, the timing of mitotic events, and aneuploidy. These parameters are more commonly investigated in non-equid mammalian species, therefore, the parameters which indicate embryo quality in the horse remains to be fully elucidated. The overall objective of this dissertation was to optimize the *in vitro* production (IVP) of equine embryos by understanding the consequences of errors that can arise during pre-mitotic and post-mitotic events. This was accomplished in 3 chapters. Chapter 1 is an introduction to the dissertation. Chapter 2: *Review of relevant literature* provides a review of the literature pertaining to early mammalian embryo development, knowledge gaps, and implications for equine embryo quality assessment. The specific aims of the experiments conducted in Chapter 3: *Pronuclear formation and cytoplasmic extrusion* and Chapter 4: *Aneuploidy in the early cleavage stage equine embryo* were to determine the pre- and post-mitotic events in the zygote using fluorescence microscopy, and the exact percentage of aneuploid embryos in the cleavage stage equine embryo. Currently, the general timing of pronuclear (PN) apposition and fusion is unknown, and this information is critical to bridge the gap in understanding the transition from the PN phase to first cleavage. We found that *in vitro* PN formation is delayed by more than 6 hours compared to previous observations of PN in the *in vivo* equine model. The sperm head is still intact at 12 hours post intracytoplasmic sperm injection (ICSI). Additionally, cytoplasmic extrusion (CE) is a pre-cleavage event unique to the horse, and previous studies have shown that CE is a critical event in equine embryo development and occurs as it is associated with developmental success. While, CE has also been described as a fragmentation event, there was little previous evidence that the extruded material contains DNA. Using fluorescence microscopy, we confirmed that no DNA was present in the extruded CE material and at this moment, the zygote was at the metaphase of mitosis.

In Chapter 4, euploid and aneuploid blastomeres were determined by single-cell sequencing for the first time in the horse. To accomplish this, embryos were removed from culture between days 2 and 3 of embryo culture following ICSI. Because embryonic endpoints were unknown, a prediction model using machine learning using time-lapse data from Chapter 3 was used to determine if the embryos would have failed or survived to blastocyst stage, and whether the early developmental stages were predictive of aneuploidy. According to the results from the sequencing data and prediction model, the blastocyst prediction model could not distinguish embryos with a higher percentage of euploid blastomeres in the horse. The percentage of aneuploid embryos were alarmingly high (81.25%), which could be explained by the frequent multipolar divisions observed during the early cleavage divisions.

The findings from this work informs future research efforts to improve IVP practices in the horse with potential applications for improving embryo outcome predictions, selection methods as well as pregnancy outcomes.

# Chapter 1

## Introduction to the dissertation

The goal of the research in this dissertation is to elucidate the factors that lead to the demise of the equine embryo prior to the blastocyst stage using time-lapse microscopy, and to determine the influence of aneuploidy in the early cleavage stage embryo using next generation sequencing. This dissertation begins with Chapter 2 which reviews all relevant scientific literature, outlining the specific background information of the gap in knowledge that remains during the early events of horse embryo development. Then, the experiments in Chapter 3 and 4 are described which play a key role in understanding the multiple failure points in equine embryo development and potentially improve the *in vitro* production (IVP) of equine embryos for pregnancy success.

The natural timeline for equine pronuclear (PN) apposition and syngamy has never been observed or defined in real-time. Additionally, the chromosomal status during cytoplasmic extrusion (CE) is currently unknown even though it has been observed in previous studies. The timing of CE, which is unique to the horse, has been shown to be associated with blastocyst rate. It is hypothesized that CE is not a form of cellular fragmentation as seen in other mammalian species as CE is observed frequently in embryos that successfully develop to blastocyst stage. However, the extruded contents have never been imaged for DNA content, nor has its relation to the first cleavage been investigated. Defining the PN stage and CE in the horse will close the gap in the IVP of equine embryos by creating a complete timeline of events to prospectively predict blastocyst formation.

The frequency of aneuploidy and mosaicism, as well as the types of errors including subchromosomal instability, using single-cell sequencing of early cleavage stage equine embryos

will be investigated in Chapter 4. The percentage of aneuploid embryos that can arise from chromosomal segregation errors at meiosis and or mitosis are currently undefined in the horse. A prediction model will be applied to predict embryo endpoints in Chapter 4 using timepoint data collected from Chapter 3. The final chapter summarizes all the major findings of each chapter and list the main conclusions and directions of future research.



# Chapter 1

## Introduction to the dissertation

The goal of the research in this dissertation is to elucidate the factors that lead to the demise of the equine embryo prior to the blastocyst stage using time-lapse microscopy, and to determine the influence of aneuploidy in the early cleavage stage embryo using next generation sequencing. This dissertation begins with Chapter 2 which reviews all relevant scientific literature, outlining the specific background information of the gap in knowledge that remains during the early events of horse embryo development. The dissertation follows by the experiments described in Chapter 3 and 4 which play a key role in understanding the multiple failure points in equine embryo development and potentially improve the *in vitro* production (IVP) of equine embryos for pregnancy success.

The natural timeline for equine pronuclear (PN) apposition and syngamy has never been observed or defined in real-time. Additionally, the chromosomal status during cytoplasmic extrusion (CE) is currently unknown even though it has been observed in previous studies. The timing of CE, which is unique to the horse, has been shown to be associated with blastocyst rate. It is hypothesized that CE is not a form of cellular fragmentation as seen in other mammalian species as CE is observed frequently in embryos that successfully develop to blastocyst stage. However, the extruded contents have never been imaged for DNA content, nor has its relation to the first cleavage been investigated. Defining the PN stage and CE in the horse will close the gap in the IVP of equine embryos by creating a complete timeline of events to prospectively predict blastocyst formation.

The frequency of aneuploidy and mosaicism, as well as the types of errors including subchromosomal instability, using single-cell sequencing of early cleavage stage equine embryos will be investigated in Chapter 4. The percentage of aneuploid embryos that can arise from chromosomal segregation errors at meiosis and or mitosis are currently undefined in the horse. A prediction model will be applied to predict embryo endpoints in Chapter 4 using timepoint data collected from Chapter 3. The final chapter summarizes all the major findings of each chapter and list the main conclusions and directions of future research.

# Chapter 2

## Review of Relevant Literature

### *I. In vitro production in the horse (Equus ferus caballus)*

*In vitro* production (IVP) of equine embryos provides the opportunity to improve efficient utilization of genetically or economically valuable horses. In cases where mares are unable to become pregnant or maintain a pregnancy due to health reasons or age, are in active competition, must undergo emergency euthanasia, or suffered an unexpected death, IVP is the only viable option to produce offspring. IVP, in conjunction with embryo transfer to a surrogate dam, is a growing reproductive technology in the commercial horse breeding industry [1,2]. The conventional assisted reproductive techniques such as artificial insemination and subsequent embryo flushing is not only time consuming and involves multiple examinations, but in addition, the mare can typically only produce a single embryo for each reproductive cycle [2]. In conjunction with the advancement of sperm cryopreservation technologies and availability of frozen straws with only a few motile sperm being necessary for the procedure, the IVP allow production of more than one embryo in each session [3,4].

The IVP of equine embryos begins with oocyte collection from immature follicles of various sizes (5-20mm) through ovum pickup (OPU), which is also termed transvaginal aspiration, (TVA), in standing sedated mares or from surgical or postmortem harvested ovaries [4,5]. Oocytes are recovered by filtration, searched under a dissecting stereomicroscope, and then placed in holding medium overnight at room temperature. The oocytes are left in holding medium prior to maturation as it increases the likelihood of the resumption of meiosis in immature oocytes and reduces total maturation time [6,7]. *In vitro* maturation (IVM) can last from 20 to 36 hrs and matured oocytes with an expanded cumulus are then denuded. Only those that have reached the

mature metaphase II (MII) stage with a visible polar body are selected for intracytoplasmic sperm injection (ICSI) [1,8]. Equine embryos obtained using IVP typically reach the blastocyst stage at day 7 or 8 but may also form a blastocyst on day 9 or 10, which are often poorer in quality. However, *in vivo* produced embryos reach the blastocyst stage at a faster rate, with day 6 being the typical day an embryo becomes a morula or early blastocyst [9]. For this reason, it is preferred that an embryo transfer of an IVP embryo to a surrogate mare occurs 4 days post ovulation in the recipient [9].

Conventional *in vitro* fertilization (IVF) is not used in equine clinical reproductive management or in research environments due to its exceedingly low success rate that is attributable to incomplete sperm capacitation, among other unknown factors [10,11]. While equine sperm can bind to the zona pellucida of *in vitro* matured oocytes, there has been inconsistent findings of whether the sperm can undergo the acrosome reaction in preparation for fertilization [10,12,13]. Dell'Aquila et al. (1999) [11] reported that the zona pellucida of equine oocytes can harden during *in vitro* maturation (IVM), making sperm penetration impossible. Zona hardening can also prevent the expansion of equine IVP blastocysts following ICSI as they do not expand to the same extent as *in vivo* produced blastocysts [14]. Thus, despite several attempts over the years to improve the success of standard IVF, IVP in horses has been accomplished only by ICSI following *in vitro* or *in vivo* oocyte maturation.

ICSI allows the sperm to bypass the natural selection process and penetrate the oocyte by directly inserting a sperm into the ooplasm. Following OPU, estimates of IVM success is greater than 50% in equine oocytes [15,16] and the use of ICSI for IVP is similarly successful, with more than a 50% fertilization rate [17–19]. Unlike conventional IVF, ICSI can pinpoint the exact time of fertilization, which is useful for downstream analyses. Moreover, immature oocytes collected

for ICSI can be held at room temperature overnight for convenience, allowing for the control of ICSI timing based on the time the immature oocytes were first placed into maturation media [2,15].

The cryopreservation of embryos rather than oocytes is still the preferred preservation method as cryopreserving oocytes results in low efficiency and survivability in the horse [9]. IVP embryos can also be more successfully cryopreserved, or more precisely, vitrified compared to flushed *in vivo* embryos. It has been shown that *in vivo*-produced embryos that are typically larger than 300µm in diameter exhibited a higher number of dead cells following the freeze/thawing process compared to smaller embryos. It has been hypothesized this may be due to the glycoprotein-rich capsule of *in vivo* embryos that forms between days 6 and 7 after ovulation during *in vivo* development or within a few days following transfer of IVP embryos to recipient mares [20]. This capsule forms between the trophectoderm and zona pellucida and may inhibit the diffusion efficiency of cryoprotectants in larger or more mature embryos with thicker capsules [20]. Unless transferred, ICSI-produced embryos lack this capsule and hence are thought to survive better with cryopreservation [21].

While there are many advantages of producing *in vitro*-derived equine embryos in the research laboratory or for commercial purposes, even with improvements in oocyte collection, oocyte maturation, subsequent fertilization, and blastocyst formation in the past two decades, the underlying mechanisms by which some embryos do not survive and arrest, while others continue to develop and reach the blastocyst stage are poorly understood. A closer observation of equine embryo development is needed using more advanced technologies such as time-lapse microscopy and next generation sequencing to understand mitotic dynamics and to further improve IVP in horses.

## II. Early embryonic development in mammalian species

Following fertilization, the mature oocyte completes meiosis II by extruding its 2<sup>nd</sup> polar body (PB) in preparation for maternal and paternal pronuclei (PN) apposition and fusion. The presence of two PBs and/or PNs in zygotes is indicative of successful fertilization [22–25]. Following male and female PN formation, migration and apposition, the nuclear membranes of each PN break down and the parental genomes undergo unification [26,27]. In mice, PN are formed after 3-4 hrs post mating [28] and in humans this was between 3-10 hrs post IVF. Once the parental DNA is duplicated, chromosome condensation occurs to allow them to align on the metaphase plate in preparation for the first mitotic division. In equine oocytes the PN phase is difficult to visualize consistently due to high optical density under the microscope due to the high lipid content in the ooplasm [29]. The timing of this series of events has remained largely undefined for equine embryos. Embryos then undergo mitosis called ‘cleavage divisions’ whereby the cell number continues to increase without changing the overall size of the embryo.

The first cleavage in equine embryos is often preceded by what is commonly referred to as ‘cellular debris’ or ‘cytoplasmic extrusion’ (CE) [5,29,30]. CE was first recorded by Hamilton and Day (1945) [31], followed by Betteridge et al (1982) [32] and Bezard et al. (1989) [33], and can be seen in images captured by Webel et al. (1977) [34] following artificial insemination and the collection of *in vivo* fertilized embryos at various intervals. CE has not been recorded until recently using time-lapse imaging (TLM) and CE seems to be a strong predictor of blastocyst success [5,35,36].

A similar pattern of cytoplasmic content being released into the perivitelline space can occur in the embryos of other mammalian species but is better known as ‘cellular fragmentation’ or ‘micronuclei’ and is largely considered a degenerative process [37,38]. Typically, cell

fragmentation arises prior to the first mitosis when a meiotic error has been inherited from the oocyte, or during one of the first divisions in the case of a mitotic error, and often remains in close proximity to the blastomeres of the embryo [38,39]. In humans and mice, extracellular debris has been shown to negatively impact developmental potential [40,41] and in non-human primates, this is because cellular fragments can contain chromosomes [39]. Extra-nuclear membrane bound bodies, known as micronuclei can also be released into the extracellular space and remain excluded, however, Chavez and colleagues (2012) have shown that micronuclei can be reabsorbed which suggest a possible correction mechanism in human embryos [38]. While CE does resemble cellular fragmentation it may represent a different cellular process. We hypothesize that if CE in equine embryos is truly similar to cellular fragmentation in other mammals, we would observe DNA in the extruded content using fluorescence microscopy. DNA content in CE is investigated in Chapter 3 of this dissertation using fluorescence microscopy.

With the first cleavage event, the mitotic phase of the embryo has begun, and the individual cells are referred to as blastomeres. As the embryo continues to divide and reaches 8-16 blastomeres, it prepares to enter the morula stage [42]. In mice [43] and horse [44], the 8-cell stage marks the beginning of cell differentiation where the inner cell mass (ICM) subsequently becomes the fetus proper, the trophectoderm (TE) is fated to form the placenta following implantation [45,46]. When the embryo reaches more than 32 blastomeres, morula compaction occurs in which the size and volume of the multicellular mass is contracted and this is achieved through the formation of tight junctions between neighboring blastomeres [45,47]. Tight junctions are formed the cell adhesion protein called E-cadherin and migrate to the cell membrane from the cell's cytoplasm [48]. At this point, individual blastomeres are indistinguishable from one another due to cell membrane breakdown and the sharing of cellular contents. The embryo will continue to

divide, and a fluid-filled cavity called the blastocoel develops, denoting the blastocyst stage and the first lineage specification. While the inner cell mass (ICM) subsequently becomes the fetus proper, the trophectoderm (TE) is fated to form the placenta following implantation [45,46].

### III. Pronuclear (PN) formation and cytoplasmic extrusion (CE) in equine embryos

As mentioned above, PN formation in equine embryos has been previously observed at 6 and 22 hours following embryo recovery after ovulation and mating [25,29]. However, the timeline and duration of equine PN formation or apposition has never been observed or defined. While Dell'Aquila et al. (2003) has visualized pronuclei using Hoechst nuclear staining at 24 hours post-ICSI, this was beyond the predicted time for PN formation [49]. On the other hand, Meyers et al. (2019) reported that embryos which successfully develop to blastocyst stage complete the first cleavage by  $24.9 \pm 1.1$  hours following ICSI [5]. Furthermore, both Lewis et al. (2019) and Meyers et al. (2019) observed CE prior to first cleavage and its significance was that only embryos that had undergone CE immediately prior to first cleavage continued to the blastocyst stage [5,36]. Based on these studies, it is reasonable to suspect that by  $19.9 \pm 1.1$  hrs when CE occurs, it is likely that the PN membranes are breaking down and the parental genomes are undergoing unification just before the first cleavage occurs at  $24.9 \pm 1.1$  hrs.

Due to the inconsistencies in the timing of PN formation between equine embryos, a complete timeline of events of both failed and successful embryos is necessary to improve the IVP of equine embryos. This timeframe of PN formation is investigated in Chapter 3 relative to PN apposition and chromosomal status at the time of CE using time-lapse and fluorescence microscopy, respectively. Additionally, a side-by-side comparison is described in Chapter 3 using morphokinetics, or the analysis of morphology and the timing of specific mitotic events, of failed



embryos versus those that successfully progressed to the blastocyst stage is included in this chapter.

#### *IV. Time-lapse microscopy (TLM) of preimplantation development*

An uninterrupted embryo culture protocol with limited exposure to the external environment is crucial for optimal embryo development. Time-lapse microscopy (TLM) is a powerful tool to study embryo development in real-time and is integral to modern human assisted reproductive technology (ART) practices. TLM has also been used to establish a morphokinetic-based embryo analysis to understand normal preimplantation development in other mammalian species, including mice, cattle, horses, and pigs [22,50–54]. The integration of TLM in horses is still in its early stages and it was not until recently that the advantages of using TLM as a predictive tool for embryo quality were reported in equine IVP [5,36,55,56]. The use of TLM is further addressed in Chapter 3.

In human clinical studies, incorporating a temporal component in embryo grading using TLM has shown to increase implantation rates [46,52,57] of transferred embryos. However, human embryo grading that solely relies on morphological assessment for embryo selection has shown to be inadequate and is not reliable enough to improve implantation rates [51,58]. For this reason, it is important to approach grading with mitotic timing assessments as well, because morphology can be subjective and aneuploid embryos, which may display varying degrees of dysfunctionality, may remain indistinguishable from euploid embryos with normal morphology [57–60]. Therefore, in human IVP embryos, morphokinetic analysis and the detection of aneuploidy, which is the presence of abnormal chromosome numbers, is necessary to achieve a higher likelihood of pregnancy following embryo transfer [52,58,61]. In human and bovine embryos, the onset of

cleavage has been shown to be associated with aneuploidy [62,63]. Additionally, the duration of the first mitotic division and/or the time intervals between the second and third cleavage in aneuploid and mosaic embryos are more likely to deviate from cleavage times of euploid embryos [38,64].

Although TLM allows close monitoring of preimplantation development, it is important to note that there are specific limitations for equine embryos when using TLM. One drawback is that once a zygote is placed into the well of the culture dish in TLM, its orientation cannot be changed unless it is taken out of the incubator. As mentioned in section III, PNs are not typically observable in equine zygotes, so the presence of PN as a marker for fertilization success cannot reliably be used. However, 2<sup>nd</sup> polar body extrusion can be captured by the imaging system and can be used as an alternative marker for successful fertilization. This is still a challenge for equine embryos as the dark ooplasm can obscure the confirmation of a 2<sup>nd</sup> polar body and the presence of CE further hinders polar body identification in developing equine embryos. For these reasons, neither the presence of a 2<sup>nd</sup> polar body or pronuclear visualization are effective ways to confirm fertilization in horses using TLM. In order to incorporate the TLM system into equine IVP, We hypothesize that the event of CE could be used as a biological marker for fertilization instead as it can be consistently observed in embryos that cleave successfully [5]. The studies described in Chapter 3 further define the utility of CE analysis using TLM. Furthermore, the precise relationship between the timing of CE and first cleavage is unknown but is likely important for the initial cleavage in the horse as CE occurs immediately before first cleavage. It is a goal of this dissertation to determine the timing of PN and CE events for equine zygotes and these studies are described in Chapter 3.

#### V. Meiotic errors lead to aneuploidy in oocytes and embryos

Meiosis in the mammalian oocyte begins in early fetal development and, following chromosome duplication and crossing over, and becomes arrested in dictyate stage of prophase I by the time of birth [65]. Only after puberty does meiosis resumes in the oocyte and undergoes recruitment for ovulation. However, the oocyte will not complete meiosis II until fertilization occurs. The misalignment of chromosomes at metaphase I (homologous chromosomes) and/or metaphase II (sister chromatids) of meiosis can result in a gain or loss of a whole chromosome(s), also known as aneuploidy [66,67]. Chromosomal segregation errors are not limited to meiosis and can occur during mitosis following oocyte fertilization [68]. Aneuploidy is one of the primary reasons for embryo arrest or loss, and consequences are infertility and low pregnancy rates [69–71]. The incidence of aneuploidy increases by age in women and can negatively impact the fidelity of the spindle assembly checkpoint (SAC) that is critical for correcting misaligned chromosomes [69,72]. The consequences of aneuploidy at the cleavage stage embryo are currently unknown in horses.

It is important to note that chromosomal integrity in the mammalian oocyte declines with the increase in maternal age and is often due to the deterioration of cohesion. Cohesion is a protein complex that holds the homologous chromosomes attached during meiosis I and the sister chromatids together until meiosis II is complete [70,73]. The loss of cohesion over time will lead to the missegregation of chromosomes or premature sister chromatid separation (PSCS), resulting in aneuploidy [65,69,74]. Therefore, cohesion is a critical structure that can ultimately determine whether the embryo will contain the correct number of chromosomes. The mechanism of how cohesion becomes degraded with advanced maternal age remains unclear and debated in literature.

In horses, it has been determined that mares older than 14 years have a higher chance of embryo loss in comparison to younger mares (2-11 years), at 61% and 11%, respectively [75]. The frequency of meiotic aneuploidy has been reported to be higher in mares <16 years of age compared to mares that are >14 years of age (56% and 16%, respectively)[76], suggesting that a maternal age of ~15 years is associated with the onset of fertility decline in horses. The persistence of meiotic aneuploidy in the cleavage stage equine embryo is unknown and is described in Chapter 4.

As mentioned above, the oocyte becomes arrested until recruitment for ovulation occurs; the oocyte remains at prophase I and while the homologous chromosomes segregate at this point, the sister chromatids are still held together by centromeric cohesion [62]. It is thought that this prolonged arrest in conjunction with an increase in maternal age plays a large role in the degradation of cohesion over time. One hypothesis as to why cohesion degrades is due to the increased sensitivity to separase, a protease that cleaves cohesin between homologous chromosomes at anaphase I and sister chromatids at anaphase II [73]. To ensure that chromosomes stay cohesion-bound, securin, which normally binds separase, is not removed by the anaphase-promoting complex/cyclosome (APC/C) until the oocyte transitions from the MI to MII stage to prevent PSCS [73,77,78]. However, a decrease in the stability of securin with aging can be a large factor in allowing for homologous chromosome missegregation or PSCS to occur during meiosis I or II, respectively [78]. A second hypothesis is that cohesion degrades over time due to the decrease in expression of shugoshin with aging. Shugoshin is a protein that protects the centromeric cohesions between each of the sister chromatids from being removed by separase during meiosis I [79]. Similar to securin, the lack of shugoshin protecting centromeric cohesion will allow PSCS to occur [80–82]. While the effects of securin and shugoshin loss over time has

been primarily studied in non-human primates and mouse models, lower expression of shugoshin with increasing age has also been shown to occur in the horse [76].

Another factor that makes the loss of cohesion catastrophic during meiosis, resulting in aneuploidy, is the disruption of the SAC prior to anaphase. The SAC is activated during prometaphase and its role is to prevent chromosome missegregation by ensuring the proper attachment of kinetochores to microtubules [70,83]. Kinetochores are localized at the centromeric regions of chromosomes and microtubules attach to the kinetochores during metaphase I and II [84]. As more researchers investigated the SAC pathway, it has become more apparent that cohesin loss alone can prevent SAC from correcting spindle errors [70,78,85]. However, the goal of the SAC is not to detect cohesion loss, but rather to detect and correct any misplaced kinetochore attachments to the chromosomes prior to anaphase. Since the loss of centromeric cohesion will loosen the physical bond between the chromosomes and microtubules, this increases the chances of failed crossing over, which can lead to univalent chromosomes at meiosis I [70]. Moreover, the increase in the distance between chromosomes can allow for the fragmentation of kinetochores, meaning that the microtubules will attach abnormally due to the multiple kinetochore fragments interacting with microtubules [84]. These findings are contrary to the initial belief that a defective SAC was the primary cause of age-related aneuploidy in oocytes [86,87]. While the SAC is not the direct source of meiotic errors, it is greatly affected by cohesion loss and the lack of securin and shugoshin will prevent proper kinetochore-microtubule attachments, leading to nondisjunction [88]. Moreover, recent studies suggest that defects in the mitotic version of the SAC called the mitotic checkpoint complex (MCC) is at least partially responsible for mitotic errors in cleavage-stage embryos [89,90].

DNA integrity in sperm is also critical as sperm do not fully undergo the natural selection process in assisted reproduction, especially with ICSI. Excessive levels of reactive oxygen species (ROS) can induce sperm DNA fragmentation [91,92], and the transmission of abnormal genetic material can be lethal or sublethal to the embryo [93,94]. While aneuploidy during spermatogenesis occurs at a lower frequency compared to oogenesis [62,95], sperm DNA fragmentation can still increase the incidence of chromosomal abnormalities, specifically during the cleavage stage [96]. Moreover, the centrosome for the first mitotic division(s) is inherited from the sperm in most mammalian species and if defective, could provide a non-genetic means to induce aneuploidy in embryos [97].

All the described factors above can lead to low embryo survivability because they are predisposed to chromosomal errors even before fertilization. The frequency of aneuploidy and mosaicism, as well as the types of errors including subchromosomal instability, using single-cell sequencing of early cleavage stage equine embryos is described in more detail in Chapter 4.

#### *VI. Contribution of mitotic errors to embryonic aneuploidy and mosaicism*

Meiotic and/or mitotic errors can lead to: 1) fully aneuploid embryos, which can be defined as embryos with no euploid cells due to chromosomal errors that occurred at both meiosis and mitosis or 2) euploid-aneuploid mosaic embryos which are embryos affected by mitotic errors that have occurred in a euploid zygote [95,98]. Unlike meiotic errors, mitotic aneuploidy arises regardless of maternal age in humans [99,100]. If chromosome missegregation occurs at the zygote stage during the first mitotic division, it can be just as lethal to the embryo as a meiotic missegregation event since all blastomeres will be affected [101,102]. Indeed, time-lapse and live-cell imaging have confirmed that the first mitotic event is highly error prone, leading to abnormal

spindle formation and lagging chromosomes at anaphase which further increases the chances of aneuploidy [26,99]. When the chromosomal abnormality arises later in the cleavage stage of preimplantation development, this will produce a mosaic embryo containing a mixture of both euploid and aneuploid cells. Mosaicism may be sublethal to the human embryo in certain instances [99,103], but some mosaic embryos can still implant upon transfer and produce seemingly healthy offspring [104,105]. In a mouse model of chromosomal mosaicism, it was shown that the fate of aneuploid cells depends on lineage, with aneuploid fetal cells being eliminated by apoptosis and aneuploid placental cells exhibiting severe proliferative defects [106]. When mosaicism is only present in the placenta but absent from the fetus is referred to as confined placental mosaicism (CPM) [107]. While the consequences of CPM can range from preterm birth to adverse pregnancy outcomes [108] and birthweight [109], these studies have very little data on aborted cases. Evidence that the placentas of aborted foals are commonly aneuploid as well suggests that aneuploid cells cannot be simply allocated to the extraembryonic lineage for a fetus to survive [102].

### VII. Aneuploidy screening via embryo biopsy and non-invasive methods

Human embryonic aneuploidy rates of mitotic origin resulting in mosaicism have varied between 15%-90% [110] based on the method used to assess chromosome number and the number of cells biopsied [110–112]. It is thought that the incidence of mitotic errors can be predicted based on the frequency of mosaic blastomeres present in a biopsied cleavage-stage embryo [110,113], but this has proven controversial [114] and has not yet been conducted on a single-cell level in blastocysts. Mosaic aneuploidy can affect pregnancy in humans, as lower clinical pregnancy outcomes have been associated with biopsied embryos with  $\geq 50\%$  mosaicism detected by the

collection of 8-10 TE cells [103]. However, the question of whether there is potential discordance between the TE and ICM or if the biopsy is truly representative of the whole embryo remains largely unanswered [115] which is why alternative methods of aneuploidy screening continue to be investigated. Besides being able to predict which embryos might successfully progress to the blastocyst stage [116] TLM has also been used to largely distinguish aneuploid and euploid embryos at multiple stages. In humans and bovine embryo studies, the onset of cleavage has been shown to be associated with aneuploidy [62,63]. Additionally, the duration of the first mitotic division and/or the time intervals between the second and third cleavage in aneuploid and mosaic embryos are also more likely to deviate from cleavage times of euploid embryos [38,64].

In humans, aneuploidy has been shown to manifest as uneven blastomeres during the cleavage stage and can be assessed using TLM [38,113,117]. An uneven cleavage division at the 2-cell stage and 4-cell stage can result in lower implantation and pregnancy loss in humans where aneuploidy rates of uneven cleavage embryos were as high as 29.4%[113]. Gene expression analysis of aneuploid and euploid murine blastomeres have shown significant differences in the expression levels of genes associated with the SAC [71], cohesion complex subunits [81,118], and the subcortical maternal complex (SCMC) [119]. The SCMC is essential for proper formation of cytoplasmic F-actin necessary for embryo development [120] allowing for symmetrical blastomere cleavage divisions [121]. Blastomere asymmetry and aneuploidy in the cleavage stage embryo will be investigated in Chapter 4.

### VIII. Summary and conclusions

Mammalian embryo quality is often graded based on morphology [38,113,117], timing of mitotic events [46,52,57], and embryonic aneuploidy rates [110,113]. Human embryo



developmental studies rely heavily on TLM for morphokinetic assessments for embryo selection purposes [51,122–124]. Previous studies using TLM in the equine IVP embryos have been associated with developmental success, yet the post-fertilization events following PN formation and chromosomal status of CE remains unclear. The experiments in Chapter 3 were designed to address these shortcomings through methods utilizing fluorescent microscopy and TLM.

Embryonic aneuploidy can lead to developmental arrest or embryonic loss [69–71] but many aneuploid embryos can persist through pregnancy [104,105,108,109]. While aneuploidy in the horse oocyte has been previously defined using FISH [76], the persistence of meiotic aneuploidy or incidences of mitotic aneuploidy after fertilization is unknown. Chapter 4 of this dissertation investigates the exact percentage of aneuploid blastomeres using single-cell DNA sequencing. Further research is needed to improve the selection method of horse IVP embryos by incorporating morphology and/or specific cleavage times that are associated with aneuploidy.

## References

- [1] Carnevale EM. Advances in Collection, Transport and Maturation of Equine Oocytes for Assisted Reproductive Techniques. *Vet Clin North Am Equine Pract* 2016;32:379–99. doi:10.1016/J.CVEQ.2016.07.002.
- [2] Stout TAE. Clinical Application of in Vitro Embryo Production in the Horse. *J Equine Vet Sci* 2020;89. doi:10.1016/j.jevs.2020.103011.
- [3] Graham JK. Cryopreservation of stallion spermatozoa. *Vet Clin North Am Equine Pract* 1996;12:131–47. doi:10.1016/S0749-0739(17)30300-0.
- [4] Squires E. Current Reproductive Technologies Impacting Equine Embryo Production. *J Equine Vet Sci* 2020;89:102981. doi:10.1016/J.JEVS.2020.102981.
- [5] Meyers S, Burruel V, Kato M, De La Fuente A, Orellana D, Renaudin C, et al. Equine non-invasive time-lapse imaging and blastocyst development. *Reprod Fertil Dev* 2019;31:1874–84. doi:10.1071/RD19260.
- [6] Galli C, Duchi R, Colleoni S, Lagutina I, Lazzari G. Ovum pick up, intracytoplasmic sperm injection and somatic cell nuclear transfer in cattle, buffalo and horses: from the research laboratory to clinical practice. *Theriogenology* 2014;81:138–51. doi:10.1016/J.THERIOGENOLOGY.2013.09.008.
- [7] Dini P, Bogado Pascottini O, Ducheyne K, Hostens M, Daels P. Holding equine oocytes in a commercial embryo-holding medium: New perspective on holding temperature and maturation time. *Theriogenology* 2016;86:1361–8. doi:10.1016/j.theriogenology.2016.04.079.
- [8] Squires EL. Maturation and fertilization of equine oocytes. *Vet Clin North Am Equine Pract* 1996;12:31–45. doi:10.1016/s0749-0739(17)30293-6.
- [9] Hinrichs K. Assisted reproductive techniques in mares. *Reprod Domest Anim* 2018;53:4–13. doi:10.1111/rda.13259.
- [10] Leemans B, Gadella BM, Stout TAE, De Schauwer C, Nelis H, Hoogewijs M, et al. Why doesn't conventional IVF work in the horse? The equine oviduct as a microenvironment for capacitation/fertilization. *Reproduction* 2016;152:R233–45. doi:10.1530/REP-16-0420.
- [11] Dell'Aquila ME, De Felici M, Massari S, Maritato F, Minoia P. Effects of Fetuin on Zona Pellucida Hardening and Fertilizability of Equine Oocytes Matured In Vitro1. *Biol Reprod* 1999;61:533–40. doi:10.1095/biolreprod61.2.533.
- [12] Tremoleda JL, Gadella BM, Stout TAE, Colenbrander B, Bevers MM. Chapter 4 Evaluation of sperm-oocyte interaction during in vitro fertilization in the horse 2003.
- [13] Meyers SA, Liu IKM, Overstreet JW, Drobnis EZ. Induction of Acrosome Reactions in Stallion Sperm by Equine Zona Pellucida, Porcine Zona Pellucida, and Progesterone1. *Biol Reprod* 1995;52:739–44. doi:10.1093/biolreprod/52.monograph\_series1.739.
- [14] Tremoleda JL, Stout TAE, Lagutina I, Lazzari G, Bevers MM, Colenbrander B, et al. Effects of In Vitro Production on Horse Embryo Morphology, Cytoskeletal Characteristics, and Blastocyst Capsule Formation. *Biol Reprod* 2003;69:1895–906. doi:10.1095/biolreprod.103.018515.
- [15] Foss R, Ortis H, Hinrichs K. Effect of potential oocyte transport protocols on blastocyst rates after intracytoplasmic sperm injection in the horse. *Equine Vet J* 2013;45:39–43. doi:10.1111/evj.12159.
- [16] Morris LHA. The development of in vitro embryo production in the horse. *Equine Vet J* 2018;50:712–20. doi:10.1111/evj.12839.

- [17] Jacobson CC, Choi Y-H, Hayden SS, Hinrichs K. Recovery of mare oocytes on a fixed biweekly schedule, and resulting blastocyst formation after intracytoplasmic sperm injection. *Theriogenology* 2010;73:1116–26. doi:10.1016/J.THERIOGENOLOGY.2010.01.013.
- [18] Choi YH, Velez IC, Macías-García B, Riera FL, Ballard CS, Hinrichs K. Effect of clinically-related factors on in vitro blastocyst development after equine ICSI. *Theriogenology* 2016;85:1289–96. doi:10.1016/j.theriogenology.2015.12.015.
- [19] Galli C, Colleoni S, Duchi R, Lagutina I, Lazzari G. Developmental competence of equine oocytes and embryos obtained by in vitro procedures ranging from in vitro maturation and ICSI to embryo culture, cryopreservation and somatic cell nuclear transfer. *Anim Reprod Sci* 2007;98:39–55. doi:10.1016/J.ANIREPROSCI.2006.10.011.
- [20] Legrand E, Krawiecki JM, Tainturier D, Cornière P, Delajarraud H, Bruyas JF. Does the embryonic capsule impede the freezing of equine embryos? *Proc 5th Int Symp Equine Embryo Transf Havemeyer Found Monogr* 2018;3:62–5.
- [21] Ginther OJ. Equine Pregnancy: Physical interactions between uterus and conceptus. *AAEP Proc* 1998;44:73–104.
- [22] Gray D, Plusa B, Piotrowska K, Na J, Tom B, Glover DM, et al. First cleavage of the mouse embryo responds to change in egg shape at fertilization. *Curr Biol* 2004;14:397–405. doi:10.1016/j.cub.2004.02.031.
- [23] Grisart B, Massip A, Dessy F. Cinematographic analysis of bovine embryo development in serum-free oviduct-conditioned medium. *Reproduction* 1994;101:257–64. doi:10.1530/jrf.0.1010257.
- [24] Van Den Bergh M, Bertrand E, Englert Y. Second Polar Body Extrusion Is Highly Predictive for Oocyte Fertilization as Soon as 3 hr After Intracytoplasmic Sperm Injection (ICSI). vol. 12. 1995.
- [25] Bezard J, M. M, Duchamp G, Palmer E. Chronology of equine fertilisation and embryonic development in vivo and in vitro. *Equine Vet J* 2010;21:105–10. doi:10.1111/j.2042-3306.1989.tb04692.x.
- [26] Cavazza T, Politi AZ, Aldag P, Baker C, Elder K, Blayney M, et al. Parental genome unification is highly erroneous in mammalian embryos. *BioRxiv* 2020:2020.08.27.269779. doi:10.1101/2020.08.27.269779.
- [27] Schneider I. Non-rodent mammalian zygotes assemble dual spindles despite the presence of paternal centrosomes. *BioRxiv* 2020. doi:10.1101/2020.10.16.342154.
- [28] Krishna M, Generoso WM. Timing of sperm penetration, pronuclear formation, pronuclear DNA synthesis, and first cleavage in naturally ovulated mouse eggs. *J Exp Zool* 1977;202:245–52. doi:10.1002/jez.1402020214.
- [29] Enders AC, Liu IKM, Bowers J, Lantz KC, Schlafke S, Suarez S. The Ovulated Ovum of the Horse: Cytology of Nonfertilized Ova to Pronuclear Stage Ova'. vol. 37. 1987.
- [30] Milewski R, Ajduk A. Time-lapse imaging of cleavage divisions in embryo quality assessment. *Reproduction* 2017;154:R37–53. doi:10.1530/REP-17-0004.
- [31] Hamilton WJ, Day FT. Cleavage stages of the ova of the horse, with notes on ovulation. *J Anat* 1945;79:127-130.3.
- [32] Betteridge KJ, Eaglesome MD, Mitchell D, Flood PF, Beriault R. Development of horse embryos up to twenty two days after ovulation: observations on fresh specimens. *J Anat* 1982;135:191–209.
- [33] Bezard J, Magistrini M, Duchamp G, Palmer E. Chronology of equine fertilisation and

- embryonic development in vivo and in vitro. *Equine Vet J* 1989;21:105–10. doi:10.1111/j.2042-3306.1989.tb04692.x.
- [34] Webel SK, Franklin V, Harland B, Dziuk PJ. Fertility, ovulation and maturation of eggs in mares injected with HCG. *J Reprod Fertil* 1977;51:337–41. doi:10.1530/jrf.0.0510337.
- [35] Marzano G, Mastrorocco A, Zianni R, Mangiacotti M, Chiaravalle AE, Lacalandra GM, et al. Altered morphokinetics in equine embryos from oocytes exposed to DEHP during IVM. *Mol Reprod Dev* 2019:mrd.23156. doi:10.1002/mrd.23156.
- [36] Lewis N, Schnauffer K, Hinrichs K, Morganti M, Troup S, Argo C. Morphokinetics of early equine embryo development in vitro using time-lapse imaging, and use in selecting blastocysts for transfer. *Reprod Fertil Dev* 2019;31:1851–61. doi:10.1071/RD19225.
- [37] Cecchele A, Cermisoni GC, Giacomini E, Pinna M, Vigano P. Cellular and Molecular Nature of Fragmentation of Human Embryos. *Int J Mol Sci* 2022;23:1349. doi:10.3390/ijms23031349.
- [38] Chavez SL, Loewke KE, Han J, Moussavi F, Colls P, Munne S, et al. Dynamic blastomere behaviour reflects human embryo ploidy by the four-cell stage. *Nat Commun* 2012;3:1251. doi:10.1038/ncomms2249.
- [39] Daughtry BL, Rosenkrantz JL, Lazar NH, Fei SS, Redmayne N, Torkency KA, et al. Single-cell sequencing of primate preimplantation embryos reveals chromosome elimination via cellular fragmentation and blastomere exclusion. *Genome Res* 2019;29:367–82. doi:10.1101/gr.239830.118.
- [40] Daughtry BL, Chavez SL. Time-lapse imaging for the detection of chromosomal abnormalities in primate preimplantation embryos. *Methods Mol Biol* 2018;1769:293–317. doi:10.1007/978-1-4939-7780-2\_19.
- [41] Homayoun H, Zahiri S, Hemayatkhah Jahromi V, Hassanpour Dehnavi A. Morphological and morphometric study of early-cleavage mice embryos resulting from in vitro fertilization at different cleavage stages after vitrification. *Iran J Vet Res* 2016;17:55–8.
- [42] Balls M, Wild A. Early mammalian development. *Nature* 1974;251:280–1. doi:10.1038/251280b0.
- [43] Roberts RM, Yong HJ, Smith S. What Drives the Formation of Trophectoderm During Early Embryonic Development? *J Reprod Dev* 2003;52:S87–97.
- [44] Iqbal K, Chitwood JL, Meyers-Brown GA, Roser JF, Ross PJ. RNA-seq transcriptome profiling of equine inner cell mass and trophectoderm. *Biol Reprod* 2014;90. doi:10.1095/biolreprod.113.113928.
- [45] Vanderwall DK. Early Embryonic Loss in the Mare. *J Equine Vet Sci* 2008;28:691–702. doi:10.1016/j.jevs.2008.10.001.
- [46] Gardner DK, Balaban B. Assessment of human embryo development using morphological criteria in an era of time-lapse, algorithms and ‘OMICs’: is looking good still important? *Mol Hum Reprod* 2016;22:704–18. doi:10.1093/molehr/gaw057.
- [47] Biggers JD, Bell JE, Benos DJ. Mammalian Blastocyst: Transport Functions in a Developing Epithelium. *Am J Physiol* 1988;255. doi:10.1152/AJPCELL.1988.255.4.C419.
- [48] Prados FJ, Debrock S, Lemmen JG, Agerholm I. The cleavage stage embryo. *Hum Reprod* 2012;27:i50–71. doi:10.1093/humrep/des224.
- [49] Dell’Aquila ME, Albrizio M, Maritato F, Minoia P, Hinrichs K. Meiotic Competence of Equine Oocytes and Pronucleus Formation after Intracytoplasmic Sperm Injection (ICSI) as Related to Granulosa Cell Apoptosis1. *Biol Reprod* 2003;68:2065–72. doi:10.1095/biolreprod.102.009852.

- [50] Campbell A, Fishel S, Bowman N, Duffy S, Sedler M, Hickman CFL. Modelling a risk classification of aneuploidy in human embryos using non-invasive morphokinetics. *Reprod Biomed Online* 2013;26:477–85. doi:10.1016/J.RBMO.2013.02.006.
- [51] Chamayou S, Patrizio P, Storaci G, Tomaselli V, Alecci C, Ragolia C, et al. The use of morphokinetic parameters to select all embryos with full capacity to implant. *J Assist Reprod Genet* 2013;30:703–10. doi:10.1007/s10815-013-9992-2.
- [52] Motato Y, de los Santos MJ, Escriba MJ, Ruiz BA, Remohí J, Meseguer M. Morphokinetic analysis and embryonic prediction for blastocyst formation through an integrated time-lapse system. *Fertil Steril* 2016;105:376-384.e9. doi:10.1016/j.fertnstert.2015.11.001.
- [53] Sugimura S, Akai T, Imai K. Selection of viable in vitro-fertilized bovine embryos using time-lapse monitoring in microwell culture dishes. *J Reprod Dev* 2017;63:353–7. doi:10.1262/jrd.2017-041.
- [54] Mateusen B, Van Soom A, Maes DGD, Donnay I, Duchateau L, Lequarre A-S. Porcine embryo development and fragmentation and their relation to apoptotic markers: a cinematographic and confocal laser scanning microscopic study. *Reproduction* 2005;129:443–52. doi:10.1530/rep.1.00533.
- [55] Carnevale EM, Catandi GD, Fresa K. Equine Aging and the Oocyte: A Potential Model for Reproductive Aging in Women. *J Equine Vet Sci* 2020;89:103022. doi:10.1016/J.JEVS.2020.103022.
- [56] Brooks KE, Daughtry BL, Metcalf E, Masterson K, Battaglia D, Gao L, et al. Assessing equine embryo developmental competency by time-lapse image analysis. *Reprod Fertil Dev* 2019;31:1840–50. doi:10.1071/RD19254.
- [57] Kirkegaard K, Ahlström A, Ingerslev HJ, Hardarson T. Choosing the best embryo by time lapse versus standard morphology. *Fertil Steril* 2015;103:323–32. doi:10.1016/J.FERTNSTERT.2014.11.003.
- [58] Fesahat F, Montazeri F, Sheikha MH, Saeedi H, Dehghani Firouzabadi R, Kalantar SM. Frequency of chromosomal aneuploidy in high quality embryos from young couples using preimplantation genetic screening. *Int J Reprod Biomed (Yazd, Iran)* 2017;15:297–304.
- [59] Majumdar G, Majumdar A, Verma IC, Upadhyaya KC. Relationship Between Morphology, Euploidy and Implantation Potential of Cleavage and Blastocyst Stage Embryos. *J Hum Reprod Sci* 2017;10:49–57. doi:10.4103/0974-1208.204013.
- [60] Fragouli E, Alfarawati S, Spath K, Wells D. Morphological and cytogenetic assessment of cleavage and blastocyst stage embryos. *Mol Hum Reprod* 2014;20:117–26. doi:10.1093/molehr/gat073.
- [61] Alfarawati S, Fragouli E, Colls P, Stevens J, Gutiérrez-Mateo C, Schoolcraft WB, et al. The relationship between blastocyst morphology, chromosomal abnormality, and embryo gender. *Fertil Steril* 2011;95:520–4. doi:10.1016/j.fertnstert.2010.04.003.
- [62] Capalbo A, Hoffmann ER, Cimadomo D, Ubaldi FM, Rienzi L. Human female meiosis revised: New insights into the mechanisms of chromosome segregation and aneuploidies from advanced genomics and time-lapse imaging. *Hum Reprod Update* 2017;23:706–22. doi:10.1093/humupd/dmx026.
- [63] Hornak M, Kubicek D, Broz P, Hulinska P, Hanzalova K, Griffin D, et al. Aneuploidy Detection and mtDNA Quantification in Bovine Embryos with Different Cleavage Onset Using a Next-Generation Sequencing-Based Protocol. *Cytogenet Genome Res* 2017;150:60–7. doi:10.1159/000452923.
- [64] Vera-Rodriguez M, Chavez SL, Rubio C, Reijo Pera RA, Simon C. Prediction model for

- aneuploidy in early human embryo development revealed by single-cell analysis. *Nat Commun* 2015;6:7601. doi:10.1038/ncomms8601.
- [65] Yun Y, Wei Z, Hunter N. Maternal obesity enhances oocyte chromosome abnormalities associated with aging. *Chromosoma* 2019;128:413–21. doi:10.1007/s00412-019-00716-6.
- [66] Battaglia DE, Goodwin P, Klein NA, Soules MR. Fertilization and early embryology: Influence of maternal age on meiotic spindle assembly oocytes from naturally cycling women. *Hum Reprod* 1996;11:2217–22. doi:10.1093/oxfordjournals.humrep.a019080.
- [67] Rizzo M, Ducheyne KD, Deelen C, Beitsma M, Cristarella S, Quartuccio M, et al. Advanced mare age impairs the ability of in vitro-matured oocytes to correctly align chromosomes on the metaphase plate. *Equine Vet J* 2019;51:252–7. doi:10.1111/evj.12995.
- [68] Tšuiiko O, Jatsenko T, Kumar L, Grace P, Kurg A, Vermeesch JR, et al. A speculative outlook on embryonic aneuploidy: Can molecular pathways be involved? 2019. doi:10.1016/j.ydbio.2018.01.014.
- [69] Yun Y, Holt JE, Lane SIR, McLaughlin EA, Merriman JA, Jones KT. Reduced ability to recover from spindle disruption and loss of kinetochore spindle assembly checkpoint proteins in oocytes from aged mice. *Cell Cycle* 2014;13:1938–47. doi:10.4161/cc.28897.
- [70] Lagirand-Cantaloube J, Ciabrini C, Charrasse S, Ferrieres A, Castro A, Anahory T, et al. Loss of centromere cohesion in aneuploid human oocytes correlates with decreased kinetochore localization of the sac proteins Bub1 and Bubr1. *Sci Rep* 2017;7:44001. doi:10.1038/srep44001.
- [71] Pan H, Ma P, Zhu W, Schultz RM. Age-associated increase in aneuploidy and changes in gene expression in mouse eggs. *Dev Biol* 2008;316:397–407. doi:10.1016/j.ydbio.2008.01.048.
- [72] Jones KT, Lane SIR. Molecular causes of aneuploidy in mammalian eggs. *Development* 2013;140:3719–30. doi:10.1242/dev.090589.
- [73] Nabti I, Reis A, Levasseur M, Stemmann O, Jones KT. Securin and not CDK1/cyclin B1 regulates sister chromatid disjunction during meiosis II in mouse eggs. *Dev Biol* 2008;321:379–86. doi:10.1016/J.YDBIO.2008.06.036.
- [74] Cheng J-M, Li J, Tang J-X, Chen S-R, Deng S-L, Jin C, et al. Elevated intracellular pH appears in aged oocytes and causes oocyte aneuploidy associated with the loss of cohesion in mice. *Cell Cycle* 2016;15:2454–63. doi:10.1080/15384101.2016.1201255.
- [75] Carnevale EM. The mare model for follicular maturation and reproductive aging in the woman. *Theriogenology* 2008;69:23–30. doi:10.1016/j.theriogenology.2007.09.011.
- [76] Rizzo M, Preez N du, Ducheyne KD, Deelen C, Beitsma MM, Stout TAE, et al. The horse as a natural model to study reproductive aging-induced aneuploidy and weakened centromeric cohesion in oocytes. *Aging (Albany NY)* 2020;12:22220–32. doi:10.18632/aging.104159.
- [77] Marangos P, Carroll J. Securin regulates entry into M-phase by modulating the stability of cyclin B. *Nat Cell Biol* 2008;10:445–51. doi:10.1038/ncb1707.
- [78] Nabti I, Grimes R, Sarna H, Marangos P, Carroll J. Maternal age-dependent APC/C-mediated decrease in securin causes premature sister chromatid separation in meiosis II. *Nat Commun* 2017;8:15346. doi:10.1038/ncomms15346.
- [79] Vincenten N, Kuhl L-M, Lam I, Oke A, Kerr AR, Hochwagen A, et al. The kinetochore prevents centromere-proximal crossover recombination during meiosis. *Elife* 2015;4.

- doi:10.7554/ELIFE.10850.
- [80] Lee J, Kitajima TS, Tanno Y, Yoshida K, Morita T, Miyano T, et al. Unified mode of centromeric protection by shugoshin in mammalian oocytes and somatic cells. *Nat Cell Biol* 2008;10:42–52. doi:10.1038/ncb1667.
- [81] Dupont C, Harvey AJ, Armant DR, Zelinski MB, Brenner CA. Expression profiles of cohesins, shugoshins and spindle assembly checkpoint genes in rhesus macaque oocytes predict their susceptibility for aneuploidy during embryonic development. *Cell Cycle* 2012;11:740–8. doi:10.4161/cc.11.4.19207.
- [82] Lister LM, Kouznetsova A, Hyslop LA, Kalleas D, Pace SL, Barel JC, et al. Age-related meiotic segregation errors in mammalian oocytes are preceded by depletion of cohesin and Sgo2. *Curr Biol* 2010;20:1511–21. doi:10.1016/j.cub.2010.08.023.
- [83] Duncan FE, Chiang T, Schultz RM, Lampson MA. Evidence That a Defective Spindle Assembly Checkpoint Is Not the Primary Cause of Maternal Age-Associated Aneuploidy in Mouse Eggs. *Biol Reprod* 2009;81:768–76. doi:10.1095/biolreprod.109.077909.
- [84] Zielinska AP, Bellou E, Sharma N, Frombach AS, Seres KB, Gruhn JR, et al. Meiotic Kinetochores Fragment into Multiple Lobes upon Cohesin Loss in Aging Eggs. *Curr Biol* 2019;29:3749–3765.e7. doi:10.1016/j.cub.2019.09.006.
- [85] Roeles J, Tsiavaliaris G. Actin-microtubule interplay coordinates spindle assembly in human oocytes. *Nat Commun* 2019;10:4651. doi:10.1038/s41467-019-12674-9.
- [86] Jones KT. Meiosis in oocytes: predisposition to aneuploidy and its increased incidence with age. *Hum Reprod Update* 2008;14:143–58. doi:10.1093/humupd/dmm043.
- [87] Vogt E, Kirsch-Volders M, Parry J, Eichenlaub-Ritter U. Spindle formation, chromosome segregation and the spindle checkpoint in mammalian oocytes and susceptibility to meiotic error. *Mutat Res Toxicol Environ Mutagen* 2008;651:14–29. doi:10.1016/J.MRGENTOX.2007.10.015.
- [88] He Y, Li X, Gao M, Liu H, Gu L. Loss of HDAC3 contributes to meiotic defects in aged oocytes. *Aging Cell* 2019;18:e13036. doi:10.1111/accel.13036.
- [89] Wei Y, Multi S, Yang C-R, Ma J, Zhang Q-H, Wang Z-B, et al. Spindle Assembly Checkpoint Regulates Mitotic Cell Cycle Progression during Preimplantation Embryo Development. *PLoS One* 2011;6:e21557. doi:10.1371/journal.pone.0021557.
- [90] Brooks KE, Daughtry BL, Davis B, Yan MY, Fei SS, Shepherd S, et al. Molecular contribution to embryonic aneuploidy and karyotypic complexity in initial cleavage divisions of mammalian development. *Development* 2022;149. doi:10.1242/dev.198341.
- [91] Lane M, McPherson NO, Fullston T, Spillane M, Sandeman L, Kang WX, et al. Oxidative Stress in Mouse Sperm Impairs Embryo Development, Fetal Growth and Alters Adiposity and Glucose Regulation in Female Offspring. *PLoS One* 2014;9:e100832. doi:10.1371/journal.pone.0100832.
- [92] Zini A, Bielecki R, Phang D, Zenzes MT. Correlations between two markers of sperm DNA integrity, DNA denaturation and DNA fragmentation, in fertile and infertile men. *Fertil Steril* 2001;75:674–7. doi:10.1016/S0015-0282(00)01796-9.
- [93] Haghpanah T, Eslami-Arshaghi T, Afarinesh MR, Salehi M. Decreased fertilization: Human sperm DNA fragmentation and in vitro maturation of oocyte in stimulated ICSI cycles. *Acta Endocrinol (Copenh)* 2017;13:23–31. doi:10.4183/aeb.2017.23.
- [94] Kumaresan A, Das Gupta M, Datta TK, Morrell JM. Sperm DNA Integrity and Male Fertility in Farm Animals: A Review. *Front Vet Sci* 2020;7:1–15. doi:10.3389/fvets.2020.00321.

- [95] McCoy RC. Mosaicism in Preimplantation Human Embryos: When Chromosomal Abnormalities Are the Norm. *Trends Genet* 2017;33:448–63. doi:10.1016/j.tig.2017.04.001.
- [96] Middelkamp S, Van Tol HTA, Spierings DCJ, Boymans S, Guryev V, Roelen BAJ, et al. Sperm DNA damage causes genomic instability in early embryonic development. *Sci Adv* 2020;6:1–12. doi:10.1126/sciadv.aaz7602.
- [97] Sathananthan AH, Kola I, Osborne J, Trounson A, Ng SC, Bongso A, et al. Centrioles in the beginning of human development. *Proc Natl Acad Sci* 1991;88:4806–10. doi:10.1073/PNAS.88.11.4806.
- [98] Munné S, Weier HUG, Grifo J, Cohen J. Chromosome Mosaicism in Human Embryos. *Biol Reprod* 1994;51:373–9. doi:10.1095/biolreprod51.3.373.
- [99] Ford E, Currie CE, Taylor DM, Erent M, Marston AL, Hartshorne GM, et al. The first mitotic division of the human embryo is highly error-prone. *BioRxiv* 2020:2020.07.17.208744. doi:10.1101/2020.07.17.208744.
- [100] Taylor TH, Gitlin SA, Patrick JL, Crain JL, Wilson JM, Griffin DK. The origin, mechanisms, incidence and clinical consequences of chromosomal mosaicism in humans n.d. doi:10.1093/humupd/dmu016.
- [101] Lane S, Kauppi L. Meiotic spindle assembly checkpoint and aneuploidy in males versus females. *Cell Mol Life Sci* 2019;76:1135–50. doi:10.1007/s00018-018-2986-6.
- [102] Shilton C, Kahler A, Davis B, Crabtree J, Crowhurst J, McGladdery A, et al. Whole genome analysis reveals aneuploidies in early pregnancy loss in the horse. *BioRxiv* 2020:2020.02.25.964239. doi:10.1101/2020.02.25.964239.
- [103] Spinella F, Fiorentino F, Biricik A, Bono S, Ruberti A, Cotroneo E, et al. Extent of chromosomal mosaicism influences the clinical outcome of in vitro fertilization treatments. *Fertil Steril* 2018;109:77–83. doi:10.1016/j.fertnstert.2017.09.025.
- [104] Greco E, Minasi MG, Fiorentino F. Healthy Babies after Intrauterine Transfer of Mosaic Aneuploid Blastocysts. *N Engl J Med* 2015;373:2089–90. doi:10.1056/NEJMc1500421.
- [105] Fragouli E, Alfarawati S, Spath K, Babariya D, Tarozzi N, Borini A, et al. Analysis of implantation and ongoing pregnancy rates following the transfer of mosaic diploid-aneuploid blastocysts. *Hum Genet* 2017;136:805–19. doi:10.1007/s00439-017-1797-4.
- [106] Bolton H, Graham SJL, Van der Aa N, Kumar P, Theunis K, Fernandez Gallardo E, et al. Mouse model of chromosome mosaicism reveals lineage-specific depletion of aneuploid cells and normal developmental potential. *Nat Commun* 2016;7:11165. doi:10.1038/ncomms11165.
- [107] Kalousek DK. Pathogenesis of chromosomal mosaicism and its effect on early human development. *Am J Med Genet* 2000;91:39–45. doi:10.1002/(sici)1096-8628(20000306)91:1<39::aid-ajmg7>3.0.co;2-l.
- [108] Toutain J, Goutte-Gattat D, Horovitz J, Saura R. Confined placental mosaicism revisited: Impact on pregnancy characteristics and outcome. *PLoS One* 2018;13:e0195905. doi:10.1371/journal.pone.0195905.
- [109] Grati FR, Ferreira J, Benn P, Izzi C, Verdi F, Vercellotti E, et al. Outcomes in pregnancies with a confined placental mosaicism and implications for prenatal screening using cell-free DNA. *Genet Med* 2020;22:309–16. doi:10.1038/s41436-019-0630-y.
- [110] Mantikou E, Wong KM, Repping S, Mastenbroek S. Molecular origin of mitotic aneuploidies in preimplantation embryos. *Biochim Biophys Acta - Mol Basis Dis* 2012;1822:1921–30. doi:10.1016/J.BBADIS.2012.06.013.



- [111] van Echten-Arends J, Mastenbroek S, Sikkema-Raddatz B, Korevaar JC, Heineman MJ, van der Veen F, et al. Chromosomal mosaicism in human preimplantation embryos: a systematic review. *Hum Reprod Update* 2011;17:620–7. doi:10.1093/humupd/dmr014.
- [112] Starostik MR, Sosina OA, McCoy RC. Single-cell analysis of human embryos reveals diverse patterns of aneuploidy and mosaicism 2020. doi:10.1101/gr.262774.120.
- [113] Hardarson T, Hanson C, Sjögren A, Lundin K. Human embryos with unevenly sized blastomeres have lower pregnancy and implantation rates: indications for aneuploidy and multinucleation. *Hum Reprod* 2001;16:313–8. doi:10.1093/humrep/16.2.313.
- [114] Mastenbroek S, Twisk M, van Echten-Arends J, Sikkema-Raddatz B, Korevaar JC, Verhoeve HR, et al. In Vitro Fertilization with Preimplantation Genetic Screening. *N Engl J Med* 2007;357:9–17. doi:10.1056/NEJMoa067744.
- [115] Gleicher N, Albertini DF, Patrizio P, Orvieto R, Adashi EY. The uncertain science of preimplantation and prenatal genetic testing. *Nat Med* 2022;28:442–4. doi:10.1038/s41591-022-01712-7.
- [116] Wong CC, Loewke KE, Bossert NL, Behr B, De Jonge CJ, Baer TM, et al. Non-invasive imaging of human embryos before embryonic genome activation predicts development to the blastocyst stage. *Nat Biotechnol* 2010;28:1115–21. doi:10.1038/nbt.1686.
- [117] Shenoy CC, Khan Z, Coddington C, Jensen J, Daftary GS, Stewart EA, et al. Symmetry at the 4-cell stage using time-lapse imaging is correlated with embryo aneuploidy. *Fertil Steril* 2015;104:e309. doi:10.1016/j.fertnstert.2015.07.966.
- [118] Cuadrado A, Losada A. Specialized functions of cohesins STAG1 and STAG2 in 3D genome architecture. *Curr Opin Genet Dev* 2020;61:9–16. doi:10.1016/j.gde.2020.02.024.
- [119] Zhu K, Yan L, Zhang X, Lu X, Wang T, Yan J, et al. Identification of a human subcortical maternal complex. *Mol Hum Reprod* 2015;21:320–9. doi:10.1093/molehr/gau116.
- [120] Li L, Baibakov B, Dean J. A Subcortical Maternal Complex Essential for Preimplantation Mouse Embryogenesis. *Dev Cell* 2008;15:416–25. doi:10.1016/j.devcel.2008.07.010.
- [121] Yu XJ, Yi Z, Gao Z, Qin D, Zhai Y, Chen X, et al. The subcortical maternal complex controls symmetric division of mouse zygotes by regulating F-actin dynamics. *Nat Commun* 2014;5:4887. doi:10.1038/ncomms5887.
- [122] Basile N, Nogales M del C, Bronet F, Florensa M, Riqueiros M, Rodrigo L, et al. Increasing the probability of selecting chromosomally normal embryos by time-lapse morphokinetics analysis. *Fertil Steril* 2014;101:699-704.e1. doi:10.1016/j.fertnstert.2013.12.005.
- [123] Chavez SL, Loewke KE, Han J, Moussavi F, Colls P, Munne S, et al. Dynamic blastomere behaviour reflects human embryo ploidy by the four-cell stage. *Nat Commun* 2012;3. doi:10.1038/ncomms2249.
- [124] Daughtry BL, Masterson KR, Metcalf ES, Battaglia D, Fei SS, Carbone L, et al. Combining Time-Lapse Imaging and Next Generation RNA-Sequencing to assess Equine Embryo Developmental Potential. *J Equine Vet Sci* 2016;41:80–1. doi:10.1016/J.JEVS.2016.04.081.

## Chapter 3

### Pronuclear formation and cytoplasmic extrusion in the early equine embryo

#### Introduction

For most mammalian species, non-invasive assessment of embryo morphology during *in vitro* culture with limited exposure to the external environment is critical for successful embryo development. Time-lapse microscopy (TLM) is a powerful clinical tool used to study embryo development in real-time and is integral to both assisted reproductive technology (ART) in humans and clinical *in vitro* production (IVP) of agriculturally relevant embryos. Due to its practicality and clinical application, numerous research reports have used TLM to establish a morphokinetic-based embryo grading with or without an automated system to better understand embryo development in humans, mice, cattle, and pigs [1–6]. While the integration of TLM in horses is still in its early stages, TLM can be utilized as a tool to assess horse embryo quality in real-time as well [7–10].

Following fertilization by a single sperm, the mature oocyte completes meiosis II by extruding its 2<sup>nd</sup> polar body (PB) in preparation for fusion of the maternal and paternal pronuclei (PN), or syngamy. Thus, the presence of two PBs and/or PNs in zygotes is indicative of successful fertilization and observable in humans and mice using light microscopy [5,11–13]. In equine zygotes, however, PN formation is difficult to visualize due to the high lipid content and subsequent increased optical density in the ooplasm of the horse [14]. Following male and female PN formation, migration and apposition, the nuclear membranes of each PN break down and the parental genomes undergo unification [15]. Once the parental DNA is duplicated, chromosome condensation occurs to allow them to align on the metaphase plate in preparation for the first mitotic division [15]. Due to the dark ooplasm, the timing of pre-cleavage events has

remained largely undefined for equine embryos. Previous *in vivo* studies have observed PN at 6 and 22 hours post coitum [13,14] which leaves open a significant gap in knowledge about the post-fertilization stages in the horse. More specifically, the general timing of PN apposition and fusion is unknown and this information is critical to bridge the gap in understanding the transition from the PN phase to first cleavage.

Unlike non-equid mammals, the first cleavage in equine embryos is often preceded by what is commonly referred to as ‘cellular debris’ or ‘cytoplasmic extrusion’ (CE) [8,9]. In other mammalian species, ‘cellular fragmentation,’ typically arises prior to the first mitosis when a meiotic error has been inherited from the oocyte, or during early the early cleavage divisions in the case of a mitotic error [16,17]. However, CE is consistently observed in the horse and appears more uniform than cellular fragmentation. In humans, non-human primates and mice, extruded extracellular debris has been shown to negatively impact developmental potential [17–19] and, at least in non-human primates, this is because cellular fragments can contain chromosomes [17]. For equids, CE is an event where cytoplasmic debris is extruded from the ooplasm into the perivitelline space [9,14,20] and thus, it is not surprising that CE has been noted as fragmentation in equine zygotes due to its granular appearance [10,21]. Currently, we do not know if the extruded material in the horse contains DNA, but we hypothesize that if CE is truly a form of fragmentation, then we would observe DNA in the extruded content using fluorescence microscopy. As a morphological marker, CE has been associated with successful cleavage in equine embryos since CE always precedes first cleavage [8,9] and the timing of CE is associated with blastocyst success in horses [8,9,22]. CE is not an artifact nor is it observed only in *in vitro* produced embryos; it was first recorded by Hamilton and Day (1945) [23], followed by Betteridge et al (1982) [24] and Bezard et al. (1989) [25], and can be seen in images captured by Webel et al. (1977) [26] following

natural mating or artificial insemination and flushing of the oviducts at various intervals. The precise timeline for the appearance of CE in real-time has not been defined until recently using TLM [8,9].

The natural timeline for equine PN apposition and syngamy has never been observed in real-time and we assessed the timing of these events in this chapter. Although CE in some instances has been called ‘fragmentation’, it is also thought to be associated with successful cleavage and blastocyst formation, indicating that the contents of the extruded material in CE should be further examined. Here, we determined the chromosomal status of the embryo at CE to understand the orientation of the parental chromosomes relative to PN appearance and disappearance as well as the first cleavage. Defining the PN stage and chromosome status prior to and during CE will close the gap in equine IVP by creating a complete timeline of events to prospectively predict which embryo will cleave and reach the blastocyst stage.

## **Materials and Methods:**

### *Live mares:*

Ten university-owned mixed and light breed mares (6-15 years) were used in these experiments. They were housed in group paddocks, with *ad libitum* access to water and hay, at the Center for Equine Health (CEH), University of California, Davis and all procedures were approved by the Institutional Animal Care and Use Committee (IACUC).

### *Oocyte collection and in vitro maturation:*

Oocytes of follicles that are 5-25mm in diameter were collected from sedated standing mares (transvaginal oocyte aspiration; TVA) as we have previously described [9]. Additional cumulus

oocyte complexes (COCs) were provided by Auburn University and Oklahoma State University. Once COCs were recovered from the mare they were held at room temperature in commercial holding medium (EquiPro Holding Medium, Minitube USA) for 19 to 21 hours. COCs were then transferred from holding media and were washed 4 times in 25 $\mu$ l drops of maturation media, and then cultured in a final dish (2-3 COCs per 25 $\mu$ l drop) under light mineral oil (Fujifilm) at 38.2°C, 5.8% CO<sub>2</sub>, 5% O<sub>2</sub> and 89.2% N<sub>2</sub> for 24-26 hrs. Maturation medium was comprised of 54% Dulbecco's modified Eagle's medium (DMEM)/F12, 25 $\mu$ g ml<sup>-1</sup> gentamicin (Sigma), 10  $\mu$ l ml<sup>-1</sup> insulin transferrin selenium (ITS), 10% dominant stimulated follicle follicular fluid, 8.8 mU ovine FSH (National Hormone and Peptide Program), 1.1mU ml<sup>-1</sup> porcine somatotropin (Harbor UCLA Research and Education Institute) and 6.0% fetal bovine serum (FBS, F2442, Sigma). For shipped COCs, they were recovered in holding media and transferred into maturation media as described above. All COCs and oocytes were handled under a dissecting microscope (Leica Microsystems).

#### *In vitro maturation and culture:*

Following maturation, oocytes that reached metaphase II were selected for ICSI based on presence of one polar body following cumulus cell removal confirmed under the dissecting microscope. For this, COCs were placed in commercial oocyte handling medium (G-MOPS, Vitrolife) with 10% fetal bovine serum (FBS) (F2442, Sigma, USA), containing 0.2% hyaluronidase (Sigma) for 2 minutes and cumulus cells were removed by micro-pipetting (140-170 $\mu$ m, Cook Medical) COC's repeatedly. Frozen sperm from a single stallion was thawed using a 30-minute swim up method as previously described [9] in commercial buffered media (G-MOPS, Vitrolife) with 10% FBS.

#### *Intracytoplasmic sperm injection (ICSI):*

ICSI was done under 5  $\mu$ l drop (1 oocyte per drop) of buffered media, G-MOPS with 10% FBS, and 2 $\mu$ l of sperm from the swim-up was placed in a 5 $\mu$ l drop of 7% polyvinylpyrrolidone PVP (Origio Inc, Cooper Surgical) under light mineral oil with a stage warmer set to 38.2°C. Sperm with normal morphology were immobilized by scoring the tail with the microinjection pipette (G18090, Cook Medical) in the drop of PVP. The single immobilized sperm was then injected into the oocyte. ICSI was done using an Olympus IX70 inverted brightfield micromanipulation microscope with Narishige micromanipulators and an Eppendorf CellTram oil microinjector.

*Time-lapse monitoring of equine embryos:*

Injected oocytes were transferred to the Miri<sup>®</sup>TL imaging incubator using a CultureCoin<sup>®</sup> (Esco Technologies) embryo dish. A schematic of this dish is shown in **Figure 3.1**. Each well contained 25 $\mu$ l of culture media (54% DMEM/F-12 (Fisher Scientific), 40% Global media (Origio Inc, Cooper Surgical), 6% FBS, 10mL ITS solution (Sigma, USA), and 0.1mM sodium pyruvate (Sigma, USA) overlaid with 3.5mL light mineral oil. Embryos were then monitored continuously with non-invasive time-lapse imaging using the Miri<sup>®</sup>TL software with image-capture set to every 5 minutes at 38.2°C under 5.8% CO<sub>2</sub>, 5%O<sub>2</sub> and 89.2% N<sub>2</sub>. On day 4, the dish and media were changed and cultured until blastocyst stage. Individual time-lapse images were assembled by the Miri<sup>®</sup>TL software into AVI movies for retrospective analysis. Each image was captured in 5 focal planes using an IW single red LED (635 nm) with total light exposure of 0.064s per captured image using a Zeiss 20x objective that is specialized for 635nm illumination. The morphological time points are shown in **Figure 3.3** where the number after ‘t’ refers to the exact number of blastomeres present at that stage.

Immunolabeling of zygotes at different PN phases:

Zygotes were removed from the individual wells in the CultureCoin at 12, 14, 16, and 18 hrs post ICSI for PN visualization and at 20 and 21 hours for determining the chromosome status when CE was complete. The timing of CE onset to the completion of CE was assessed by TLM (**Figure 3.2**). For fluorescence microscopy, zygotes were fixed at room temperature in 4% paraformaldehyde in D-PBS (Sigma) containing 0.1% gentamicin (Fisher Scientific) for 40 minutes. All zygotes were processed under a dissecting microscope. Embryos were then permeabilized at room temperature in 0.1 % Triton X-100 (Sigma) in DPBS-gentamicin for 30 minutes and then incubated in blocking buffer in 10% normal donkey serum in DPBS-gentamicin 0.1% Triton X-100 for 2 hours [9]. Fixed zygotes were then incubated with monoclonal anti- $\alpha$ -Tubulin-FITC antibody (1:100) (F2168, Sigma) diluted in PBS 0.1% TX containing 1% FBS for 30 min at room temperature. Then zygotes were washed 3 times in washing buffer (D-PBS with 0.1% gentamicin). Nuclei were stained in 10 mg/ml of bisbenzimidazole (Hoechst 33258, Fisher Scientific) for 20 min and washed 3 times in washing buffer before mounting. For mounting, 10  $\mu$ l of an antifade medium, Vectashield (Vector Laboratories), was used. Mounted zygotes were imaged using the Zeiss Observer Imaging inverted microscope and processed using Zen Blue<sup>®</sup> software (Carl Zeiss, Inc.).

Statistical analysis:

Welch's t-test with R software [28] was used to compare the timing of embryonic events of two groups: (1) embryos that successfully developed to blastocyst stage, and (2) embryos that failed to reach blastocyst stage. The embryonic events compared were the: exact timings of the onset of CE (CE start), CE completion (CE end) to the eighth cleavage event (t2-t8). The morphological time

points are shown in **Figure 3.3**. Embryo morphology was only analyzed up to t8 for both groups to minimize variability and the effect of small sample sizes.  $P < 0.05$  was considered significant.

## **Results:**

### *Chromosome status of equine zygotes*

When characterizing the pronuclear phase of equine embryo development by nuclear and microtubule staining at 12, 14, 16, and 18 hrs post ICSI, we observed that the sperm had not yet undergone decondensation at 12 hrs post ICSI ( $n=5/6$ , 83%), male pronuclei (PN) had formed by 14 hrs post ICSI ( $n=2/4$ , 50%), and individual spindles formed around the parental genomes by 18 hrs post ICSI ( $n=1/3$ , 33%) (**Figure 3.4**). We observed 5 of the 6 zygotes processed for fluorescence imaging with the sperm head still intact and the female PN beginning to form nucleolar precursor bodies [15] at 12 hours post ICSI. While the image acquired at 18 hrs may not be a correct representation of proper parental spindle alignment ( $n=1/3$ ), we should consider abnormal parental spindle assembly as a potential contributor to aneuploidy [29,30]. With our visualization of dual spindle formation through fluorescence microscopy at 18 hrs post ICSI, we confirm that dual spindles also forms in the horse zygote which was previously only confirmed in other mammalian species, including the mouse [31] and cattle [15,32]).

### *DNA is not detectable within the granular material of CE*

After 20 to 21 hrs post-ICSI, CE completion was confirmed in the zygotes through TLM (**Figure 3.2**). This was within the window of CE reported in previous studies [8,9] and was also within our established morphological timepoints in experiment 3 (see below). During this period, the zygote appears to be in the metaphase stage of mitosis based on the presence of the metaphase plate



(**Figure 3.5**). Thus, the DNA within zygotes ( $n=3$ ) was stained using Hoechst 33258 and the polar bodies could be observed amongst the material that was extruded into the perivitelline space. However, of the 3 zygotes imaged, there was no fluorescence observed in the remaining granular material, suggesting that DNA was not contained within the CE.

*Immunofluorescence of cleavage-stage embryos without CE reveals multipolar spindle formation*

An embryo ( $n=1$ ) cleaved into 3 cells without undergoing cytoplasmic extrusion (CE) (**Figure 3.6**). It is likely that the embryo did not align parental spindles after the PN stage and proceeded to divide based on our observations of the normal metaphase plate at CE (**Figure 3.5**) and the abnormally distanced parental spindles undergoing anaphase in **Figure 3.4** at 18 hrs post ICSI.

*Timing of early cleavage events differs between arrested embryos and blastocysts*

Embryos that failed to reach the blastocyst stage showed significant delays in the early developmental stages following ICSI. For all embryos that developed to blastocyst stage ( $n=47$ ), the CE start time was  $16.64\pm 4.8$  hrs post ICSI (**Table 3.1**), which was 5 hours earlier than the CE start time for embryos that failed to reach blastocyst stage ( $n=84$ ) (**Figure 3.7**,  $P<0.05$ ). The first cleavage ( $t_2$ ) was completed by  $26.68\pm 5.7$  hrs for embryos that reached blastocyst stage. In comparison, embryos that arrested prior to the blastocyst stage reached  $t_2$  7 hours later ( $33.75\pm 1.0$  hrs,  $P<0.05$ ). In addition, arrested embryos were delayed by 15 hours when  $t_4$  was complete in embryos that formed blastocysts ( $P<0.05$ ). At  $t_5$ , embryos that reached blastocyst had completed  $t_5$  11 hours earlier compared to embryos that did not reach blastocyst stage ( $P<0.05$ ).

## Discussion:

To assess the relationship between PN formation and disappearance with CE, the initiation of cleavage divisions, and successful blastocyst formation, three experiments were conducted: 1) an assessment of PN between 12-18 hours post ICSI to identify the timing of PN apposition and fusion (n=19), 2) an assessment of chromosomal status at CE (n=3) and 3) a comparison of CE timing in embryos that failed to develop to blastocyst stage (n=84) versus those that developed to blastocyst stage (n=47). For experiment 1, the 12-18 hour window was chosen based on existing data of observed equine PN formation between 6 and 22 hours post coitum [13,14]. This decision to select this time window also factored in findings from cattle, since PNs are regularly observed under light microscopy in bovine zygotes and completely formed by 10 hours after IVF [33]. In addition, the first cleavage occurs after 24 hrs in bovine embryos [34], which is similar in timing in the horse [8,9], and helped direct when the equine zygotes should be removed for analysis.

In comparison to *in vivo* fertilized embryos [13], our fluorescence imaging of the PN stage shows the 6+ hr delay in that the sperm decondensation event had not yet occurred by 12 hrs post ICSI in the IVP embryos [13,14]. This could explain some differences in the developmental timing from fertilization between the *in vivo* and *in vitro* embryos [35]. By 16 hours, PN have completed migration and are in apposition. Chromosome clustering can be observed at this time, and chromosome clustering has been recorded in bovine zygotes previously as well [15]. Interestingly, at 18 hrs the dual spindles have formed but the parental genomes are in anaphase. According to Cavazza et al. (2020), if the dual spindles have not overlapped before undergoing anaphase the likelihood of the embryo undergoing abnormal chromosomal segregation is very high resulting in multinucleated blastomeres during mitosis [31]. Two additional images were taken at 18 hrs post ICSI, and in both instances, the parental genomes had overlapped and were at different stages of

anaphase. We also observed abnormal multipolar spindles in an embryo ( $n=1$ ) that did not undergo CE. Multipolar spindles in humans can arise from abnormal centrosomes [36] and will lead to chromosome missegregation [37,38]. Further experiments are needed to determine if chromosomal or spindle abnormalities are observed in embryos that cleave but do not exhibit CE.

Even though Dell'Aquila et al. (2003) [39] had visualized pronuclei using Hoechst nuclear staining at 24 hours post ICSI, when compared to time-lapse data which showed first cleavage at ~24 hrs [8,9], this was beyond the predicted time for PN formation. And as shown in our data, there are significant developmental delays between embryos that reached the blastocyst stage and embryos that arrest prior to this and is consistent with previous research that also used TLM in equine embryos [8,9]. Our visualization of CE at 20 and 21 hrs post ICSI was confirmed through TLM. This was within the window of CE reported in previous studies [8,9] and was also within our established morphological timepoints in experiment 3. With the defined progression from PN apposition, fusion to the onset of CE, the zygote with PN at 24 hours observed by Dell'Aquila et al. (2003) [39] was likely delayed.

Even before the use of TLM, CE was observed in zygotes recovered from the infundibulum post natural breeding or artificial insemination [23,40,41] but it has been referred to as 'granular material'[23,40] 'fragmentation'[10,21], 'cytoplasmic debris' or 'cytoplasmic extrusion'[8,9] as well as a 'pre-mitotic event'[9]. Despite its variability in naming, all the events described above had occurred prior to first cleavage. To address the uncertainty in describing this event, we used fluorescence microscopy to determine if CE is similar to or distinct from cellular fragmentation that occurs in other mammals. We found that there is no DNA contained within the granular material extruded into the perivitelline space as previously postulated [10]. Cellular fragmentation in other mammalian species can occur before first cleavage and has been shown to be arise due to

a meiotic error [16,17]. Thus, even though CE occurs before first cleavage and there was no DNA in the extruded material, there is still the possibility that fragmentation can occur in the horse before the first cleavage. Therefore, distinctions between fragmentation and CE should be made to eliminate confusion for the purpose of embryo grading. Additionally, future studies are necessary to identify the exact cellular contents that are being extruded, and what the purpose or function of extruding cytoplasmic content into the perivitelline space means for the embryo. For this experiment, our limitation was the small sample size for assessing the DNA content in CE. To fully confirm the absence of DNA fragments in CE, DNA sequencing must be conducted.

Developmental delays during early cleavage divisions in the horse have been observed using TLM in previously studies [8,9] where the timing of CE can offset the timing of first cleavage [9]. More specifically, Meyers et al. (2019) observed a delay in CE timing of 4 hours between successful and failed blastocysts and our data confirms that CE delay is associated with embryo outcome. However, in this study, we observed a longer delay of 5 hours in CE timing between the two groups. Even though our data supports the early cleavage time with blastocyst success, there is a possibility that these embryos may contain chromosomal abnormalities as shown in our fluorescence imaging at 18 hr post ICSI. In humans, both early and delayed cleavage times are associated with embryonic aneuploidy [42,43]. Perhaps the abnormal parental spindle alignment observed at 18 hrs post ICSI in the equine zygote can also lead to a delay in development as observed in the bovine model. The delay at anaphase as shown in bovine zygotes was a consequence non-polarized chromosome condensation at the pronuclear interface [15]. Additionally, in the mouse model where microtubules were intentionally depolymerized using Nocodazole, parental spindles that failed to align were more likely to segregate into multinucleated blastomeres [31]. While we do not know if aneuploidy was also the leading cause of delay or arrest

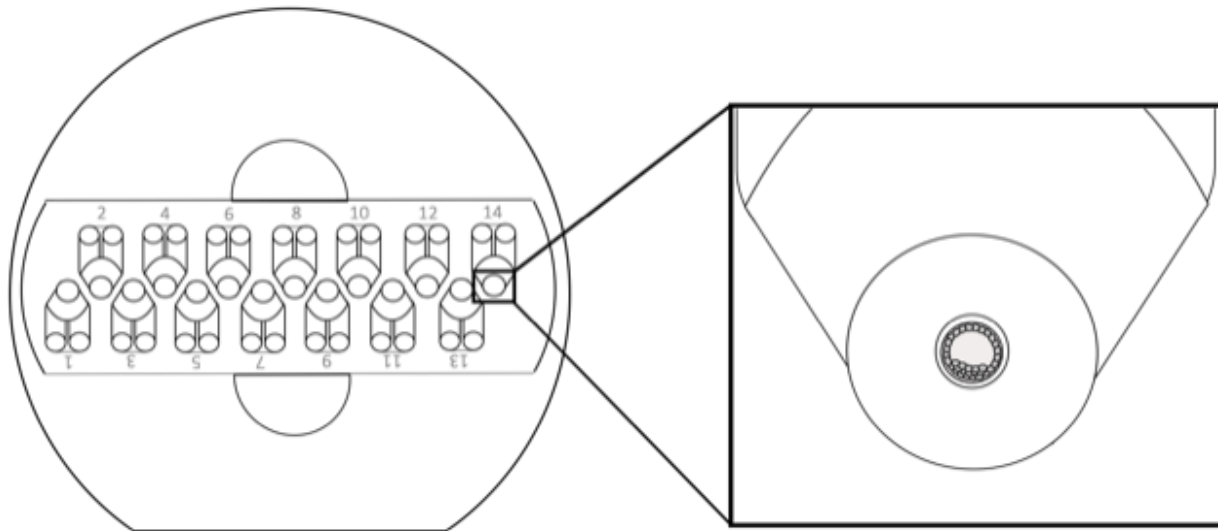
for embryos that did not survive to the blastocyst stage in this study, the experiments presented in Chapter 4 of this dissertation suggest that equine cleavage stage embryos suffer from a high incidence of aneuploidy that may determine embryo fate.

In human clinical studies, incorporating a temporal component in addition to morphological assessment, known as morphokinetics, in embryo grading using TLM has shown to increase implantation rates [3,44,45] of transferred embryos. However, embryo grading that solely relies on morphological assessment for embryo selection has shown to be inadequate as it is subjective and is not reliable enough to improve implantation rates in humans [2,46]. While early equine embryonic events have been previously established using TLM, here we have identified the timing of PN apposition and fusion, as well as the association between CE and mitosis which are all pre-cleavage events that had not been visualized in real-time before this study. Our findings show that similar to other mammalian species [15,31,32] a delay can occur starting parental genome unification before CE. And as a strong predictor of blastocyst success, CE should be incorporated alongside other mitotic morphokinetic parameters to improve pregnancy success in the horse.

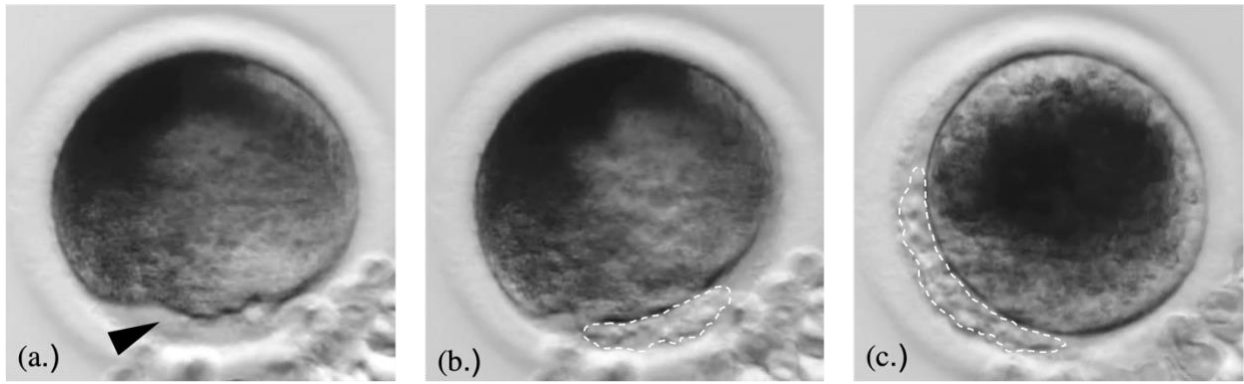
In conclusion, we have identified timeframe of PN apposition and fusion and found that the timing of CE is a critical for equine embryo developmental success. We also found that CE in equine embryos likely differs from cellular fragmentation in other species since DNA was not detected in the extruded material, but a greater number of embryos should be evaluated to confirm this finding since whole and/or partial chromosomes were observed in the fragments from only ~18% of non-human primate embryos [17]. The earlier CE timing was associated with blastocyst formation, and embryos that undergo CE later in development will likely continue to be delayed, eventually leading to embryonic demise. In future work, the timing of embryonic events will be

associated with the occurrence of aneuploidy in IVP horse embryos to further improve the IVP of equine embryos for pregnancy success.

## Tables and Figures

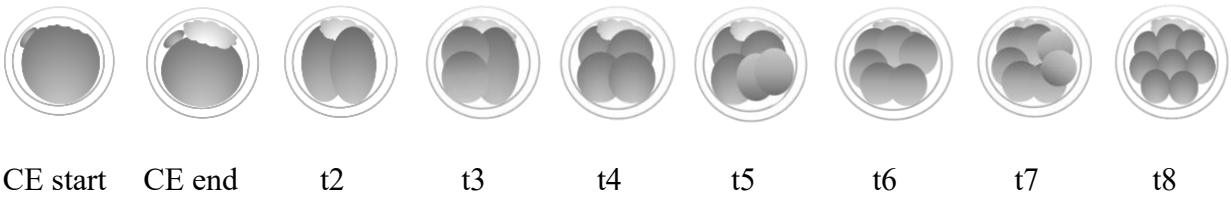


**Figure 3.1:** A schematic of the CultureCoin (Esco Technologies) that was used for embryo culture in TLM. Each CultureCoin can culture up to 14 embryos, and here we show what a well with an embryo looks like in the last well. Each well holds 25 $\mu$ L of embryo culture media with a 3.5mL light mineral oil overlay. (From: Meyers et al. *Equine non-invasive time-lapse imaging and blastocyst development*. *Reproduction, Fertility and Development*, 2019, 31, 1874–1884 <https://doi.org/10.1071/RD19260>)

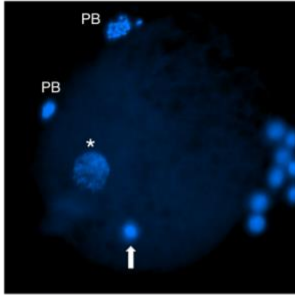
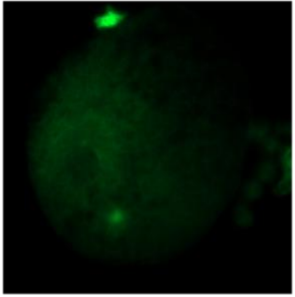
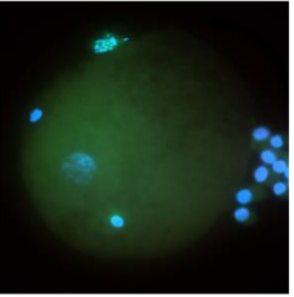
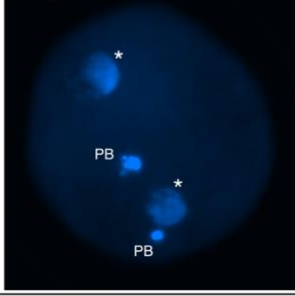
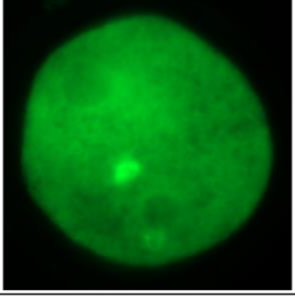
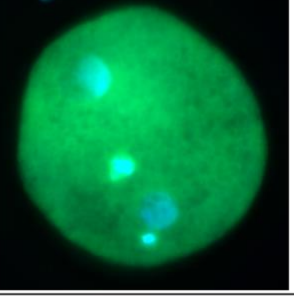
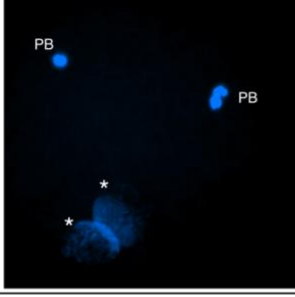
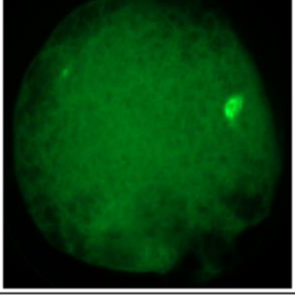
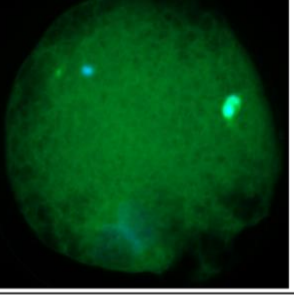
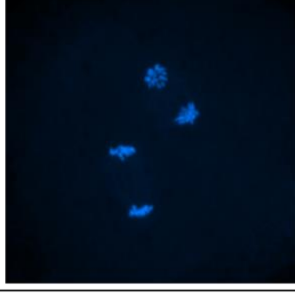
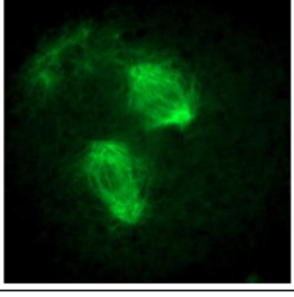
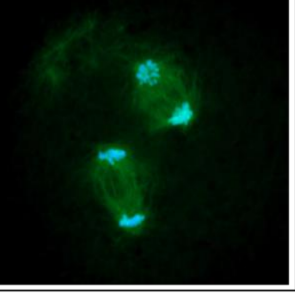


**Figure 3.2:** Cytoplasmic extrusion (CE) in the horse embryo. This sequence of images shows: (a.) the beginning of CE with the uneven rippling of the ooplasm (black arrow), (b.) the cytoplasmic content beginning to be released into the perivitelline space (white dashed line), and finally (c.) the completion of CE with no more cytoplasmic content being released into the perivitelline space.





**Figure 3.3:** Embryonic stages that were assessed using the Miri TL time-lapse system. CE onset (CE start) and completion of CE (CE end) was tracked in the zygote followed by the timing of each cleavage event (t2 to t8). Note that the number after t refers to the number of blastomeres present after each division.

Hrs post ICSI	Hoechst 33258	FITC	Merged	Times observed
12 hrs				5/6
14 hrs				2/4
16 hrs				4/6
18 hrs				1/3

**Figure 3.4:** Immunofluorescence of tubulin using monoclonal anti- $\alpha$ -Tubulin-FITC antibody (green) and nuclear staining (blue) using Hoechst 33258. 12 hrs post ICSI: the sperm head (white arrow) was still intact and had not undergone decondensation. At 14 hrs post ICSI: both male and female pronuclei (PN) had formed. At 16 hrs post ICSI: the male and female PN in apposition and by 18 hrs post ICSI: the parental genomes had formed individual spindles. PB, polar body; \*, pronuclei

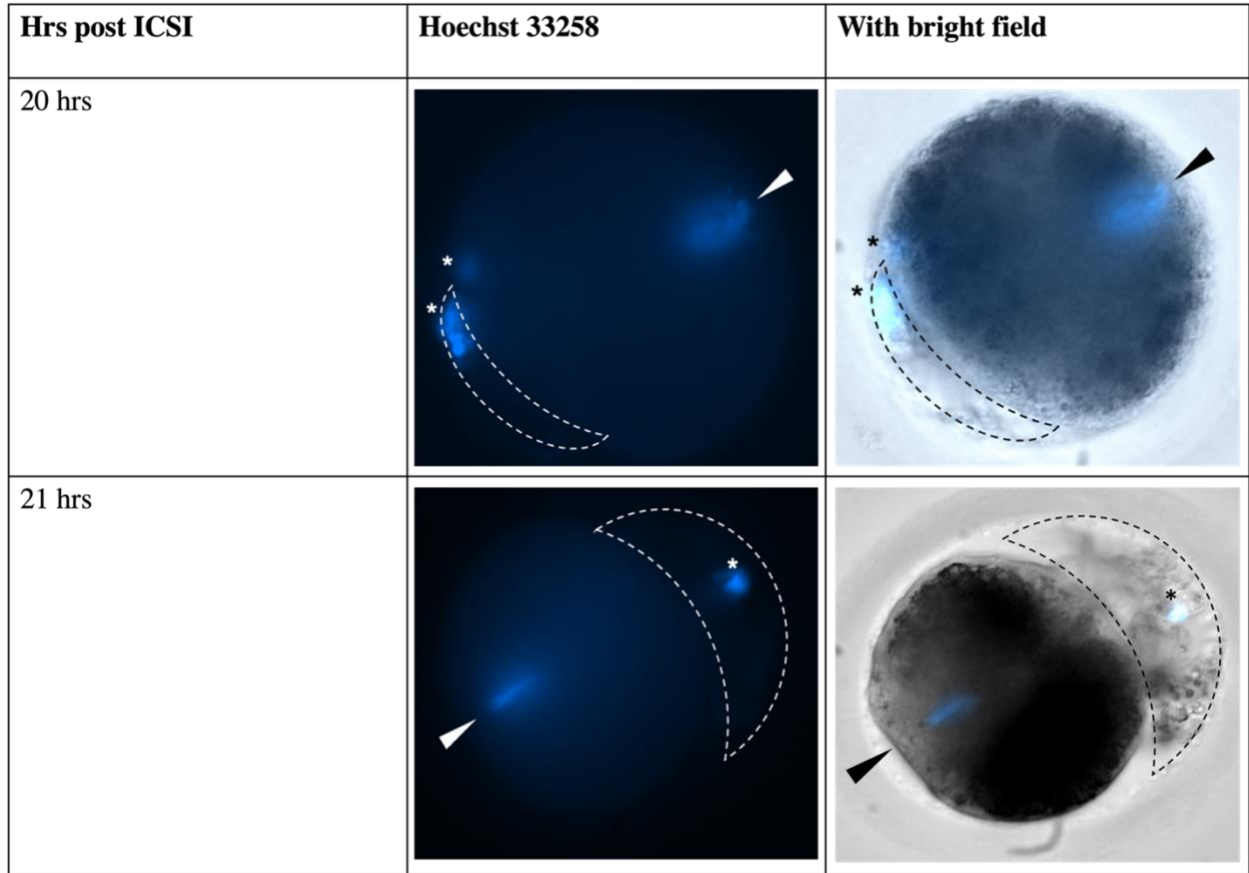


**Figure 3.5:** An equine embryo at 20 hours and 21 hours post ICSI imaged using fluorescence and bright field microscopy with Hoechst 33258 staining. The metaphase plate is present (black arrows) prior to the embryo's first mitotic cleavage event. Extruded material in the perivitelline space is indicated by a dotted line. Other than the polar bodies (PB) indicated by an asterisk, there is no sign of fragmentation as there is no DNA fluorescing in the extruded material after CE.

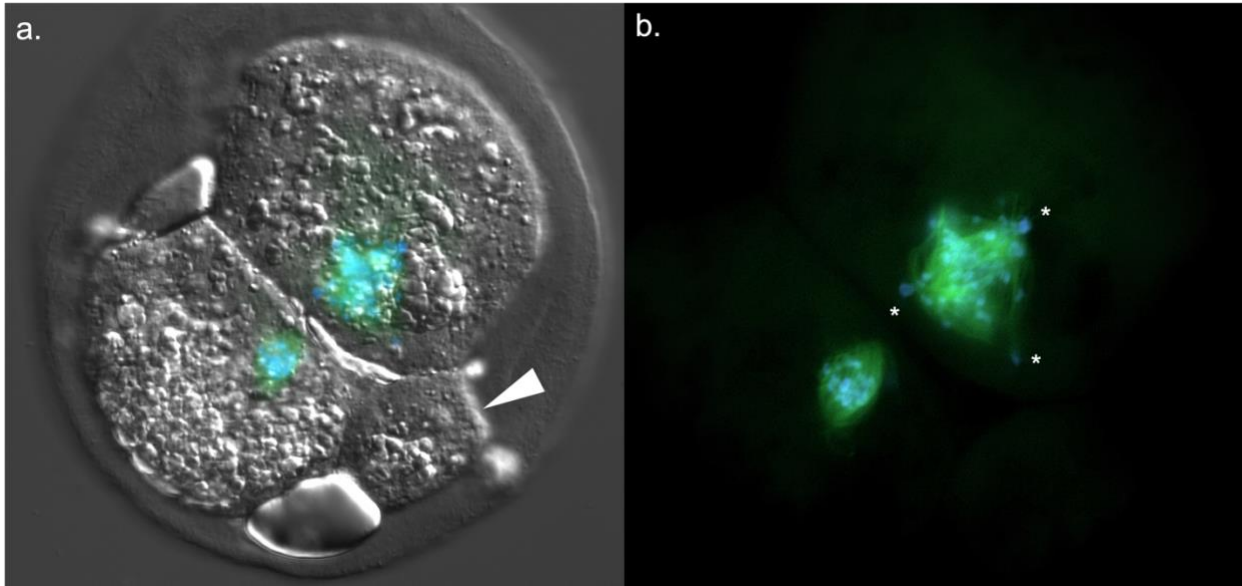


**Figure 3.6:** Fluorescence microscopy of an embryo that lacked CE revealed a multipolar spindle in one blastomere. (a.) Phase contrast microscopy of a 3-cell embryo that did not undergo CE, which is a critical developmental marker. One of the cells appeared smaller (white arrow) than the other blastomeres. Immunofluorescent staining of the embryo with tubulin using a monoclonal anti- $\alpha$ -Tubulin-FITC antibody (green) and DNA staining (blue) using Hoechst 33258 demonstrated that the small blastomere contained no DNA. (b.) The same embryo without phase contrast microscopy revealed multipolar spindle formation in one of the larger blastomeres. \*mark spindle poles.

### Comparison of embryonic events between Blast and NonBlast groups

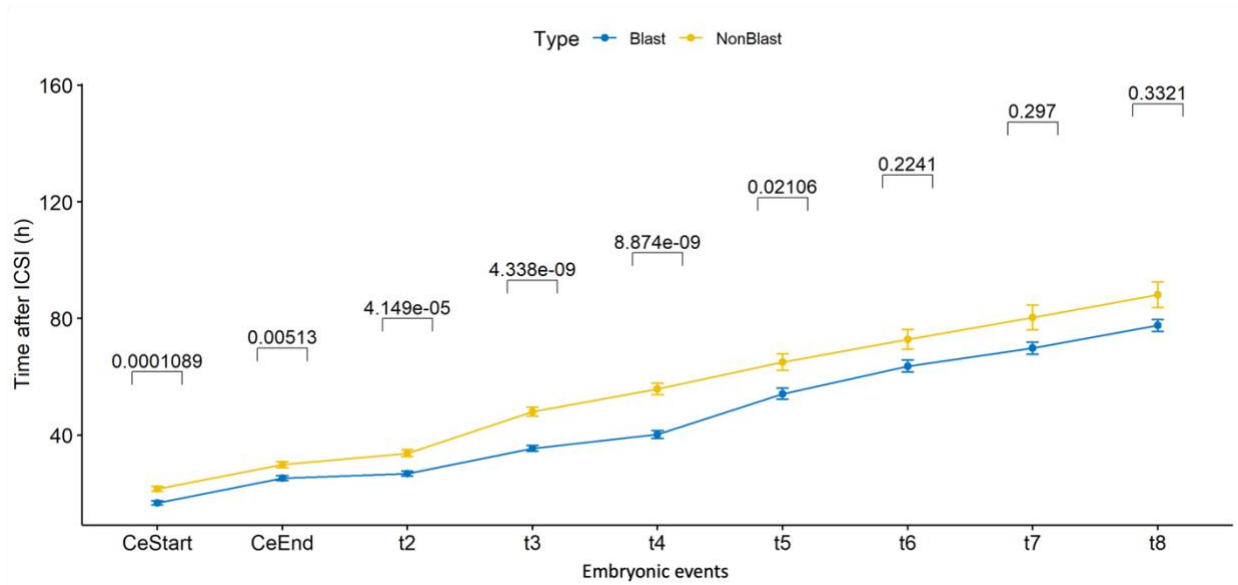


**Figure 3.7:** A line plot comparing the 2 groups based on time from ICSI and embryonic events. Embryos that developed to blastocyst stage (Blast) between CE start to t5 are significantly different from embryos that failed to develop to blastocyst (NonBlast) ( $P < 0.05$ ). Refer to Table 1 for the means of each timepoint for the 2 groups.

**Table 3.1: Embryonic events of embryos that developed to blastocyst stage (blastocyst) and embryos that did not develop to blastocyst stage (no blastocyst)**

CE, Cytoplasmic extrusion; t2-t8, 2- to 8-cell stage

<b>Embryo stage</b>	<b>CE start</b>	<b>CE end</b>	<b>t2</b>	<b>t4</b>	<b>t5</b>	<b>t6</b>	<b>t7</b>	<b>t8</b>
Blastocyst Mean±s.e.m (hrs)	16.64±4.8 (n=47)	25.14±5.8 (n=47)	26.68±5.7 (n=47)	40.17±8.9 (n=47)	54.18±1.3 (n=47)	63.63±1.4 (n=47)	69.79±1.4 (n=47)	77.58±1.4 (n=47)
No Blastocyst Mean±s.e.m (hrs)	21.53±7.5 (n=84)	29.84±8.3 (n=84)	33.75±1.0 (n=84)	55.79±1.8 (n=84)	65.03±1.8 (n=43)	72.76±2.0 (n=35)	80.31±2.3 (n=28)	88.17±2.1 (n=24)

## References

- [1] Campbell A, Fishel S, Bowman N, Duffy S, Sedler M, Hickman CFL. Modelling a risk classification of aneuploidy in human embryos using non-invasive morphokinetics. *Reprod Biomed Online* 2013;26:477–85. doi:10.1016/J.RBMO.2013.02.006.
- [2] Chamayou S, Patrizio P, Storaci G, Tomaselli V, Alecci C, Ragolia C, et al. The use of morphokinetic parameters to select all embryos with full capacity to implant. *J Assist Reprod Genet* 2013;30:703–10. doi:10.1007/s10815-013-9992-2.
- [3] Motato Y, de los Santos MJ, Escriba MJ, Ruiz BA, Remohí J, Meseguer M. Morphokinetic analysis and embryonic prediction for blastocyst formation through an integrated time-lapse system. *Fertil Steril* 2016;105:376–384.e9. doi:10.1016/j.fertnstert.2015.11.001.
- [4] Sugimura S, Akai T, Imai K. Selection of viable in vitro-fertilized bovine embryos using time-lapse monitoring in microwell culture dishes. *J Reprod Dev* 2017;63:353–7. doi:10.1262/jrd.2017-041.
- [5] Gray D, Plusa B, Piotrowska K, Na J, Tom B, Glover DM, et al. First cleavage of the mouse embryo responds to change in egg shape at fertilization. *Curr Biol* 2004;14:397–405. doi:10.1016/j.cub.2004.02.031.
- [6] Mateusen B, Van Soom A, Maes DGD, Donnay I, Duchateau L, Lequarre A-S. Porcine embryo development and fragmentation and their relation to apoptotic markers: a cinematographic and confocal laser scanning microscopic study. *Reproduction* 2005;129:443–52. doi:10.1530/rep.1.00533.
- [7] Carnevale EM, Catandi GD, Fresa K. Equine Aging and the Oocyte: A Potential Model for Reproductive Aging in Women. *J Equine Vet Sci* 2020;89:103022. doi:10.1016/J.JEVS.2020.103022.
- [8] Lewis N, Schnauffer K, Hinrichs K, Morganti M, Troup S, Argo C. Morphokinetics of early equine embryo development in vitro using time-lapse imaging, and use in selecting blastocysts for transfer. *Reprod Fertil Dev* 2019;31:1851–61. doi:10.1071/RD19225.
- [9] Meyers S, Burrue V, Kato M, De La Fuente A, Orellana D, Renaudin C, et al. Equine non-invasive time-lapse imaging and blastocyst development. *Reprod Fertil Dev* 2019;31:1874–84. doi:10.1071/RD19260.
- [10] Brooks KE, Daughtry BL, Metcalf E, Masterson K, Battaglia D, Gao L, et al. Assessing equine embryo developmental competency by time-lapse image analysis. *Reprod Fertil Dev* 2019;31:1840–50. doi:10.1071/RD19254.
- [11] Grisart B, Massip A, Dessy F. Cinematographic analysis of bovine embryo development in serum-free oviduct-conditioned medium. *Reproduction* 1994;101:257–64. doi:10.1530/jrf.0.1010257.
- [12] Van Den Bergh M, Bertrand E, Englert Y. Second Polar Body Extrusion Is Highly Predictive for Oocyte Fertilization as Soon as 3 hr After Intracytoplasmic Sperm Injection (ICSI). vol. 12. 1995.
- [13] Bezaud J, M. M, Duchamp G, Palmer E. Chronology of equine fertilisation and embryonic development in vivo and in vitro. *Equine Vet J* 2010;21:105–10. doi:10.1111/j.2042-3306.1989.tb04692.x.
- [14] Enders AC, Liu IKM, Bowers J, Lantz KC, Schlafke S, Suarez S. The Ovulated Ovum of the Horse: Cytology of Nonfertilized Ova to Pronuclear Stage Ova. vol. 37. 1987.
- [15] Cavazza T, Politi AZ, Aldag P, Baker C, Elder K, Blayney M, et al. Parental genome unification is highly erroneous in mammalian embryos. *BioRxiv* 2020:2020.08.27.269779. doi:10.1101/2020.08.27.269779.

- [16] Chavez SL, Loewke KE, Han J, Moussavi F, Colls P, Munne S, et al. Dynamic blastomere behaviour reflects human embryo ploidy by the four-cell stage. *Nat Commun* 2012;3:1251. doi:10.1038/ncomms2249.
- [17] Daughtry BL, Rosenkrantz JL, Lazar NH, Fei SS, Redmayne N, Torkenczy KA, et al. Single-cell sequencing of primate preimplantation embryos reveals chromosome elimination via cellular fragmentation and blastomere exclusion. *Genome Res* 2019;29:367–82. doi:10.1101/gr.239830.118.
- [18] Daughtry BL, Chavez SL. Time-lapse imaging for the detection of chromosomal abnormalities in primate preimplantation embryos. *Methods Mol Biol* 2018;1769:293–317. doi:10.1007/978-1-4939-7780-2\_19.
- [19] Homayoun H, Zahiri S, Hemayatkhah Jahromi V, Hassanpour Dehnavi A. Morphological and morphometric study of early-cleavage mice embryos resulting from in vitro fertilization at different cleavage stages after vitrification. *Iran J Vet Res* 2016;17:55–8.
- [20] Milewski R, Ajduk A. Time-lapse imaging of cleavage divisions in embryo quality assessment. *Reproduction* 2017;154:R37–53. doi:10.1530/REP-17-0004.
- [21] Morris LHA. The development of in vitro embryo production in the horse. *Equine Vet J* 2018;50:712–20. doi:10.1111/evj.12839.
- [22] Marzano G, Mastrorocco A, Zianni R, Mangiacotti M, Chiaravalle AE, Lacalandra GM, et al. Altered morphokinetics in equine embryos from oocytes exposed to DEHP during IVM. *Mol Reprod Dev* 2019:mrd.23156. doi:10.1002/mrd.23156.
- [23] Hamilton WJ, Day FT. Cleavage stages of the ova of the horse, with notes on ovulation. *J Anat* 1945;79:127-130.3.
- [24] Betteridge KJ, Eaglesome MD, Mitchell D, Flood PF, Beriault R. Development of horse embryos up to twenty two days after ovulation: observations on fresh specimens. *J Anat* 1982;135:191–209.
- [25] Bezard J, Magistrini M, Duchamp G, Palmer E. Chronology of equine fertilisation and embryonic development in vivo and in vitro. *Equine Vet J* 1989;21:105–10. doi:10.1111/j.2042-3306.1989.tb04692.x.
- [26] Webel SK, Franklin V, Harland B, Dziuk PJ. Fertility, ovulation and maturation of eggs in mares injected with HCG. *J Reprod Fertil* 1977;51:337–41. doi:10.1530/jrf.0.0510337.
- [27] Foss R, Ortis H, Hinrichs K. Effect of potential oocyte transport protocols on blastocyst rates after intracytoplasmic sperm injection in the horse. *Equine Vet J* 2013;45:39–43. doi:10.1111/evj.12159.
- [28] R. Core Team. R: A language and environment for statistical computing 2018.
- [29] Battaglia DE, Goodwin P, Klein NA, Soules MR. Fertilization and early embryology: Influence of maternal age on meiotic spindle assembly oocytes from naturally cycling women. *Hum Reprod* 1996;11:2217–22. doi:10.1093/oxfordjournals.humrep.a019080.
- [30] Rizzo M, Ducheyne KD, Deelen C, Beitsma M, Cristarella S, Quartuccio M, et al. Advanced mare age impairs the ability of in vitro-matured oocytes to correctly align chromosomes on the metaphase plate. *Equine Vet J* 2019;51:252–7. doi:10.1111/evj.12995.
- [31] Reichmann J, Nijmeijer B, Hossain MJ, Eguren M, Schneider I, Politi AZ, et al. Dual-spindle formation in zygotes keeps parental genomes apart in early mammalian embryos. *Science (80- )* 2018;361:189–93. doi:10.1126/science.aar7462.
- [32] Schneider I. Non-rodent mammalian zygotes assemble dual spindles despite the presence of paternal centrosomes. *BioRxiv* 2020. doi:10.1101/2020.10.16.342154.
- [33] Parrish JJ. Bovine in vitro fertilization: in vitro oocyte maturation and sperm capacitation



- with heparin. *Theriogenology* 2014;81:67–73. doi:10.1016/j.theriogenology.2013.08.005.
- [34] Dinnyés A, Lonergan P, Fair T, Boland MP, Yang X. Timing of the first cleavage post-insemination affects cryosurvival of in vitro-produced bovine blastocysts. *Mol Reprod Dev* 1999;53:318–24. doi:10.1002/(SICI)1098-2795(199907)53:3<318::AID-MRD7>3.0.CO;2-O.
- [35] Hinrichs K. Assisted reproductive techniques in mares. *Reprod Domest Anim* 2018;53:4–13. doi:10.1111/rda.13259.
- [36] Balczon R, Bao L, Zimmer WE, Brown K, Zinkowski RP, Brinkley BR. Dissociation of centrosome replication events from cycles of DNA synthesis and mitotic division in hydroxyurea-arrested Chinese hamster ovary cells. *J Cell Biol* 1995;130:105–15. doi:10.1083/jcb.130.1.105.
- [37] Chatzimeletiou K, Morrison EE, Prapas N, Prapas Y, Handyside AH. Spindle abnormalities in normally developing and arrested human preimplantation embryos in vitro identified by confocal laser scanning microscopy. *Hum Reprod* 2005;20:672–82. doi:10.1093/humrep/deh652.
- [38] McCoy RC, Newnham LJ, Ottolini CS, Hoffmann ER, Chatzimeletiou K, Cornejo OE, et al. Tripolar chromosome segregation drives the association between maternal genotype at variants spanning PLK4 and aneuploidy in human preimplantation embryos. *Hum Mol Genet* 2018;27:2573–85. doi:10.1093/hmg/ddy147.
- [39] Dell'Aquila ME, Albrizio M, Maritato F, Minoia P, Hinrichs K. Meiotic Competence of Equine Oocytes and Pronucleus Formation after Intracytoplasmic Sperm Injection (ICSI) as Related to Granulosa Cell Apoptosis1. *Biol Reprod* 2003;68:2065–72. doi:10.1095/biolreprod.102.009852.
- [40] Betteridge KJ, Eaglesome MD, Mitchell D, Flood PF, Beriault R. Development of horse embryos up to twenty two days after ovulation: observations on fresh specimens. *J Anat* 1982;135:191.
- [41] Ball BA, Little T V, Weber JA, Woods GL. Survival of Day-4 embryos from young, normal mares and aged, subfertile mares after transfer to normal recipient mares. *J Reprod Fertil* 1989;85:187–94.
- [42] Tesarik J, Greco E, Mendoza C. Late, but not early, paternal effect on human embryo development is related to sperm DNA fragmentation. *Hum Reprod* 2004;19:611–5. doi:10.1093/humrep/deh127.
- [43] Iffanolida PA, Wiweko B, Yuningsih T, Mansyur E, Muna N, Mutia K, et al. Late embryo cleavage as an indicator of chromosome aneuploidy by pre-implantation genetic screening. *J Phys* 2018;42049. doi:10.1088/1742-6596/1073/4/042049.
- [44] Gardner DK, Balaban B. Assessment of human embryo development using morphological criteria in an era of time-lapse, algorithms and 'OMICS': is looking good still important? *Mol Hum Reprod* 2016;22:704–18. doi:10.1093/molehr/gaw057.
- [45] Kirkegaard K, Ahlström A, Ingerslev HJ, Hardarson T. Choosing the best embryo by time lapse versus standard morphology. *Fertil Steril* 2015;103:323–32. doi:10.1016/J.FERTNSTERT.2014.11.003.
- [46] Fesahat F, Montazeri F, Sheikhha MH, Saeedi H, Dehghani Firouzabadi R, Kalantar SM. Frequency of chromosomal aneuploidy in high quality embryos from young couples using preimplantation genetic screening. *Int J Reprod Biomed (Yazd, Iran)* 2017;15:297–304.

## Chapter 4

## **Aneuploidy in the early cleavage stage equine embryo**

### **Introduction**

Meiosis in the oocyte begins in early fetal development and by birth, oocytes become arrested in the dictyate stage of prophase I [1], a state in which they remain until puberty. Following puberty, meiosis resumes in the oocyte that undergoes recruitment for ovulation, but it will not complete meiosis II until fertilization occurs. During meiosis, misalignment of chromosomes at metaphase I (homologous chromosomes) and/or metaphase II (sister chromatids) can result in a gain or loss of a whole chromosome(s), which is also known as aneuploidy [2,3]. Abnormal chromosomal numbers are one of the primary reasons for embryo arrest or loss, resulting in infertility and low pregnancy rates in many mammals [4–6]. Chromosomal segregation errors, however, are not limited to meiosis and can occur during mitosis following oocyte fertilization [7]. The frequency of aneuploidy increases with age in women and can negatively impact the fidelity of the spindle assembly checkpoint that is essential for correcting misaligned chromosomes [4,8]. However, the incidence and underlying cause(s) of aneuploidy during the early cleavage stages are currently unknown in the horse.

Research has shown that oocyte chromosomal integrity declines with the increase in maternal age of mammals and is often due to the deterioration of cohesion. Cohesion is a protein complex that holds the homologous chromosomes attached during meiosis I and the sister chromatids together until meiosis II is complete [5,9]. The loss of cohesion over time will lead to the missegregation of chromosomes or premature sister chromatid separation (PSCS), resulting in aneuploidy [1,4,10]. While cohesion is a critical structure that can ultimately determine whether the embryo will be able to successfully maintain the correct number of chromosomes, exactly how cohesion becomes degraded with advanced maternal age is still under much investigation.

Regardless of the mechanism, meiotic and/or mitotic errors can lead to: 1) aneuploid embryos, which can be defined as embryos with no euploid cells due to chromosomal errors that occurred at both meiosis and mitosis or 2) euploid-aneuploid mosaic embryos which are embryos affected by mitotic errors that have occurred in a euploid zygote [11,12].

Unlike meiotic errors, mitotic aneuploidy can occur regardless of maternal age in humans [13,14]. If chromosome missegregation occurs at the zygote stage during the first mitotic division, it can be just as lethal to the embryo as a meiotic missegregation event since all blastomeres will be affected [15,16]. Indeed, time-lapse and live-cell imaging have confirmed that the first mitotic event is highly error prone, leading to abnormal spindle formation and lagging chromosomes at anaphase and further increasing the chances of aneuploidy [13,17]. When the chromosomal abnormality arises later in the cleavage stage of preimplantation development, this will produce a mosaic embryo containing a mixture of both euploid and aneuploid cells. Mosaicism may be sublethal to the human embryo in certain instances [13,18], but some mosaic embryos can still implant upon transfer and produce seemingly healthy offspring [19,20]. In a mouse model of chromosomal mosaicism, it was shown that the fate of aneuploid cells depends on lineage, with aneuploid fetal cells being eliminated by apoptosis and aneuploid placental cells exhibiting severe proliferative defects [21]. However, evidence that the placentas of aborted foals are commonly aneuploid suggests that the allocation of aneuploid cells to the extraembryonic lineage for a fetus does not always guarantee survival to term [16].

In horses, it has been determined that mares older than 14 years have a higher chance of embryo loss in comparison to younger mares (2-11 years), at 62% and 11%, respectively [22]. Similar to humans, the frequency of meiotic aneuploidy has been reported to be higher in mares  $\geq 16$  years of age compared to younger mares  $\leq 14$  years (56% and 16%, respectively) [23].

Moreover, while human studies of embryonic aneuploidy have moved from fluorescence *in-situ* hybridization (FISH) of a limited number of chromosomes [24] to whole-genome methods using array comparative genomic hybridization (aCGH) or next generation sequencing [25–27], the detection of aneuploidy in equine oocytes or embryos has only been previously investigated using FISH [23,28]. Besides assessing all chromosomes, these techniques can detect subchromosomal losses and/or gains that would have otherwise been missed by FISH.

The underlying mechanisms by which some embryos do not survive and arrest, while others continue in development and reach the blastocyst stage are poorly understood. The aim of this study was to investigate the frequency of aneuploidy that may persist in the early cleavage stage between day 1 and day 3 post fertilization by distinguishing chromosomal errors of meiotic and/or mitotic origin using single-cell next generation sequencing. Additionally, we applied time-lapse data collected in Chapter 3 to train the blastocyst prediction model to assess possible endpoints of sequenced embryos.

## **Materials and Methods:**

### *Animals, oocyte collection and in vitro maturation:*

Cumulus oocyte complexes (COCs) from antral follicles were shipped from Auburn University ( $n=19$ ) and Oklahoma State University ( $n=28$ ). They were shipped in an insulated container to hold temperatures  $\sim 22^{\circ}\text{C}$  (Equitainer; Hamilton Thorne Biosciences). COCs were then transferred from holding media (EquiPro, Minitube USA) and were washed 4 times in 25 $\mu\text{l}$  drops of maturation media which was prepared in the lab and was comprised of 54% Dulbecco's modified Eagle's medium (DMEM)/F12, 25 $\mu\text{g ml}^{-1}$  gentamicin (Sigma), 10  $\mu\text{l ml}^{-1}$  insulin transferrin selenium (ITS), 10% dominant stimulated follicle follicular fluid, 8.8 mU ovine FSH (National

Hormone and Peptide Program), 1.1mU ml<sup>-1</sup> porcine somatotropin (Harbor UCLA Research and Education Institute) and 6.0% fetal bovine serum (FBS, F2442, Sigma). and then cultured in a final dish (2-3 COCs per 25 ul drop) under light mineral oil (Fujifilm) at 38.2°C, 5.8% CO<sub>2</sub>, 5% O<sub>2</sub> and 89.2% N<sub>2</sub> for 24-26 hrs.

*In vitro maturation and oocyte disaggregation:*

Following maturation, oocytes that reached metaphase II (identified by the presence of a polar body) were selected for ICSI based on presence of one polar body following cumulus cell removal. Briefly, COCs were placed in commercial oocyte handling medium (G-MOPS, Vitrolife) with 10% fetal bovine serum (FBS) (F2442, Sigma, USA), containing 0.2% hyaluronidase for 2 minutes and cumulus cells were removed by micro-pipetting (140-170µm, Cook Medical) COC's repeatedly.

*Sperm preparation and intracytoplasmic sperm injection (ICSI):*

Frozen sperm from a single stallion with proven IVP success was thawed using a 30-minute swim up method as previously described [30] in commercial buffered media (G-MOPS, Vitrolife) with 10% FBS. Intracytoplasmic sperm injection (ICSI) was done under buffered media, G-MOPS with 10% FBS, and selected sperm was placed in 7% PVP (Origio Inc, Cooper Surgical) under light mineral oil with a stage warmer set to 38.2°C. Each oocyte was placed in a 5 µl drop of buffered G-MOPS with 10% FBS, and 2µl of sperm from the swim-up method described above was placed in a 5µl drop of 7% polyvinylpyrrolidone PVP (Origio Inc, Cooper Surgical) under light mineral oil. Sperm with normal morphology were immobilized using the microinjection pipette (G18090, Cook Medical) to score the tail in the drop of PVP. Then a single immobilized sperm was then

injected into the oocyte. ICSI was done using an Olympus IX70 inverted brightfield micromanipulation microscope equipped with Narishige micromanipulators, Eppendorf CellTram oil microinjectors and a stage warmer which was set to 38.2°C.

*Embryo culture:*

Injected oocytes were then transferred to the Miri<sup>®</sup>TL imaging incubator using a CultureCoin<sup>®</sup> (Esco Technologies) embryo dish within ten minutes of sperm injection. Each well contained 25µl of culture media (54% DMEM/F-12 (Fisher Scientific), 40% Global (Origio Inc, Cooper Surgical), 6% FBS, 10mL mL<sup>-1</sup> ITS solution (Sigma, USA), and 0.1mM sodium pyruvate (Sigma, USA) overlaid with 3.5mL light mineral oil. Embryos were then monitored continuously with non-invasive time-lapse imaging using the Miri<sup>®</sup>TL software with an image-capture set to every 5 minutes at 38.2°C under 5.8% CO<sub>2</sub>, 5%O<sub>2</sub> and 89.2% N<sub>2</sub>. On day 4, the dish and media were changed and cultured until blastocyst stage or up to day 11 post ICSI. Individual time-lapse images were assembled by the Miri<sup>®</sup>TL software into AVI movies for retrospective analysis. Each image was captured in 5 focal planes using an IW single red LED (635 nm) with total light exposure of 0.064s per captured image using a Zeiss 20x objective in the Miri<sup>®</sup>TL that was specialized for 635nm illumination.

*Embryo disaggregation:*

Cleavage stage embryos were removed from time-lapse imaging on 1-, 2- or 3-days post ICSI and were disaggregated into individual blastomeres as previously described [31] using a dissecting microscope. Briefly, the zona pellucida (ZP) was removed using acidified Tyrode's solution (Millipore) and washed in Ca<sup>2+</sup> and Mg<sup>2+</sup> free phosphate buffer saline (PBS) with 0.1% bovine

serum albumin (A3294, Sigma Aldrich). ZP-free embryos were disaggregated manually in GMOPS (Vitrolife, Sweden) with 10% fetal bovine serum (F2442, Sigma). Individual blastomeres were then washed in Ca<sup>2+</sup> and Mg<sup>2+</sup> free PBS and stored in sterile PCR tubes (Fisher Scientific). All samples were flash frozen on dry ice and stored at -80°C.

### Fibroblast isolation

Full-thickness 4-cm<sup>2</sup> skin specimens were excised using a biopsy punch and aseptic technique from the neck of a standing sedated horse. The collected biopsies were washed and transported to the lab using the transport medium, containing 1X Hank's balanced salt solution (HBSS) with phenol red (Thermo Fisher Scientific), penicillin and streptomycin (100 U/ml and 100 µg/ml, respectively; Thermo Fisher Scientific), 250 mg/L of gentamicin sulfate (Cellgro, Mediatech Inc., Herndon, VA), and 0.25 µg/ml of amphotericin B (Gibco, Carlsbad, CA)). The dermal and subcutaneous tissues were minced and placed in tubes with the gentleMACS dissociator enzyme kit (# 130-110-201; Miltenyi Biotec Inc.), following the manufacturer protocol for dissociation of human kidney using the Multi Tissue Dissociation Kit 1. Single cells were plated in Dulbecco's modified minimum essential medium (DMEM; Cellgro) with 10% ferritin-supplemented calf serum (HyClone, GE Healthcare, Chicago, IL), penicillin and streptomycin (100 U/ml and 100 µg/ml, respectively), and 0.25 µg/ml of amphotericin B (Gibco, Carlsbad, CA), and incubated at 37°C and 5% CO<sub>2</sub> until confluent.

### Whole genome amplification (WGA):

WGA of disassembled equine embryos and individual fibroblasts was performed using the SMARTer PicoPLEX Gold kit (Takara Bio Cat. #R300670) according to the manufacturer's

instructions with slight modifications. Each blastomere was lysed at 75°C for 10 min. followed by pre-amplification at 95°C for 2 min. and 12 cycles of gradient PCR with PicoPLEX pre-amp enzyme and primer mix. Pre-amplified DNA was further amplified with PicoPLEX amplification enzyme and 48 uniquely-indexed Illumina sequencing adapters provided by the kit as previously described [31]. Adapter PCR amplification consisted of a 95°C hotstart for 4 min., four cycles of 95°C for 20 sec., 63°C for 25 sec., and 72°C for 40 sec. and seven cycles of 95°C for 20 sec. and 72°C for 55 sec. Libraries were quantified with a Qubit High Sensitivity (HS) DNA assay (Life Technologies, Carlsbad, CA). Amplified DNA from each blastomere and fibroblast (50ng) was pooled into two groups and purified with AMPure® XP beads (Beckman Coulter, Indianapolis, IN). Final pooled library quality assessment was performed on a 2200 TapeStation (Agilent, Santa Clara, CA).

*Single-cell DNA sequencing (scDNA-seq):*

Each pool was sequenced on one Illumina NovaSeq 6000 run in the OHSU Massively Parallel Sequencing Shared Resource (MPSSR) and the data transferred from the MPSSR via SSH for analysis. All raw sample reads were demultiplexed and sequencing quality assessed with FastQC [32]. Illumina adapters were removed from raw reads with the sequence grooming tool, Cutadapt [33], which trimmed 15 bases on the 5' end and five bases from the 3' end, resulting in reads of 120 bp on average. Trimmed reads were aligned to the most recent equine reference genome, *EquCab3* [34], using the BWA-MEM option of the Burrows-Wheeler Alignment Tool with default alignment parameters [35]. Resulting bam files were filtered to remove alignments with quality scores below 30 ( $Q < 30$ ) as well as alignment duplicates that were likely the result of PCR artifacts



with the Samtools suite [36]. The average number of filtered and uniquely mapped sequencing reads in individual libraries was between 3.5 million (blastomeres) and 14.8 million (fibroblasts).

#### *Copy Number Variation (CNV) analysis:*

Previously, we developed our own CNV bioinformatics pipeline, whereby read counts are compared in contiguous windows across the genome between a given sample and a known euploid control [31]. This approach utilized windows of variable width, but constant read count set to 4,000 reads, to factor in the variation in “mappability” across the genome and control for potential biases from WGA as previously shown [37]. Each aneuploidy was classified as meiotic or mitotic in origin by determining whether a loss or gain of the same chromosome was detected in all blastomeres (meiotic) or if reciprocal chromosome losses and gains were observed between blastomeres (mitotic). Since CNV can be reliably assessed at a 15 Mb resolution with 0.5-1X genome coverage [38,39], we classified breaks of 15 Mb in length or larger that did not affect the whole chromosome as segmental. Chaotic aneuploidy was classified by the loss or gain of greater than four whole and/or broken chromosomes as previously described [31]. Additional classifications included cells that either failed WGA or were identified as empty due to the detection of mitochondrial DNA, but not nuclear DNA.

#### *Prediction analysis using machine learning:*

Time-lapse data for training and testing the model was obtained from Chapter 3 (n=131) to predict for blastocyst formation in the sequenced embryos (n=16). Initially, we compared the performance of each model in terms of accuracy (Logistic regression, Linear Discriminant, SVM, K Neighbors, Gradient Boosting, Random Forest, Extra Trees Classifier, XGBoost, LightGBM, and

AdaBoost[40]), and the AdaBoost classifier had the highest accuracy (70%) in predicting the correct embryo results. The trained AdaBoost model was evaluated using the equations as shown:

TPR (True Positive Rate) / Recall / Sensitivity =  $True\ Positive\ (TP)/(TP + False\ Positive\ (FP))$

Specificity =  $True\ Negative\ (TN)/(TN+FP)$

False Positive Rate =  $(1 - Specificity)/(FP)$

The model achieved an area under the curve (AUC) of 81.8% when tested with a subset of time-lapse data that was not used in the training dataset for the time points and biological timepoints: CE start, CEstart – CE end, CEstart – t2 and t2 – t3. Class probabilities were calculated per embryo prediction (threshold 0.5) to determine if the embryo would have survived to the blastocyst stage if they were not removed for whole embryo single-cell sequencing.

### Blastomere symmetry

Blastomere symmetry was determined based on the occurrence of multipolar divisions as previously shown [41]. To limit variability in blastomere analysis, one embryologist analyzed all TLM videos ( $n=16$ ) for blastomere symmetry.

### Statistical analysis:

Blastocyst prediction analysis and the incidence of blastomere (a)symmetry, euploidy versus aneuploidy, and multipolar divisions were analyzed using Chi-square in R [42] and  $P<0.05$  was considered statistically significant.

### **Results:**

### *Assessment of whole and segmental aneuploidy in equine blastomeres*

To our knowledge, no study has yet examined CNV in blastomeres from equine embryos using a whole-genome method that unlike DNA-FISH [23,28] examines all chromosomes and can detect sub-chromosomal losses and/or gains that would have otherwise been overlooked. Therefore, we applied our scDNA-seq strategy to 16 equine embryos cultured for 1-3 days and disassembled into individual cells for a total of 85 blastomeres with between 2 and 12 blastomeres collected per embryo. As shown in **Figure 4.1**, we observed 7 embryos with at least one euploid blastomere and it should be noted that the other blastomere(s) from three of these embryos contained segmental errors only (embryo 4, 6 and 14), which warrants further investigation at a higher sequencing coverage to confirm these as segmental errors. In contrast, several embryos were comprised of blastomeres that were entirely aneuploid (embryo 3 and 5) or likely to be completely aneuploid given that some blastomeres failed WGA or were considered empty (embryo 2, 8, 9, and 15). The remaining embryos contained a mixture of chromosomally normal and abnormal blastomeres and thus, were classified as euploid-aneuploid mosaic (embryo 1, 12, 13, and 16) or exhibited a combination of whole and segmental chromosome segregation errors (embryo 7, 10, and 11). Chaotic aneuploidy, or the loss and/or gain of more than 4 chromosomes, was observed in one or more blastomeres of most embryos (~68.8%; N=11/16), which along with empty blastomeres, has been shown to be a product of multipolar divisions in other mammals [31,43,44].

### *Identification of meiotic and mitotic chromosome mis-segregation events*

Once the chromosomal contents of each embryo were reconstructed using the CNV information from all blastomeres, we detected the meiotic loss of chromosome 22 in three blastomeres from embryo 5 (**Figure 4.2**). No copies of chromosome 22 were observed in the fourth blastomere from

this embryo and when combined with the information from the other chromosomes, was classified as chaotic aneuploidy. This suggested that the complete loss of chromosome 22 was associated with additional chromosomal losses and gains. Moreover, while most mitotic errors were non-reciprocal, we identified at least one reciprocal mitotic loss and gain of chromosome 8 between two blastomeres from embryo 9 (**Figure 4.3**). The third blastomere also exhibited a loss of one copy of chromosome 8, indicating that it was the daughter cell of the blastomere with the same loss and that the mis-segregation event likely occurred at the zygote stage during the first mitotic division. Besides the loss of chromosome 8, the third blastomere also contained other whole and partial losses of different chromosomes but did not reach the level to be considered chaotic aneuploidy. Taken together, we determined that the frequency of aneuploidy originating from both meiotic and mitotic mis-segregation errors was very high at 81.25% even if the segmental errors detected in one or more blastomeres from embryos 4, 6 and 14 were confirmed by higher sequencing coverage (**Figure 4.1**).

#### *Correlation between embryo ploidy and morphology by time-lapse imaging*

After establishing the percentage of aneuploidy in equine cleavage-stage embryos, we investigated the correlation between embryo chromosomal status and certain morphological parameters in real-time using time-lapse imaging. Because cytoplasmic extrusion (CE) prior to the first mitotic division is thought to be a critical developmental marker in equine embryos, we first investigated the frequency of this phenomenon in the cleavage-stage embryos. All embryos exhibited CE prior to or during the first cleavage division (**Table 4.1**). Many of these embryos also underwent multipolar divisions at the zygote stage which was observed under Miri<sup>®</sup>TL resulting in blastomere asymmetry (**Figure 4.4a**). Moreover, 5 of these embryos exhibited extreme multipolar divisions,

dividing from 1-cell to 4- or 5-cells during the first mitotic division (**Figure 4.4b**). Lastly, at least one embryo (# 15) had multiple multipolar divisions, resulting in at least 9 visible blastomeres on day 2 rather than the typical 4 cells observed at this timepoint (**Figure 4.4c**). We also measured the time intervals of the first three mitotic divisions in each embryo based on previous findings that these imaging parameters, in conjunction with the timing and degree of cellular fragmentation, are predictive of ploidy status in cleavage stage human embryos [41] but did not observe significant differences in early mitotic timing between euploid and aneuploid equine embryos.

#### *Blastocyst prediction using machine learning is not perfect*

To predict the developmental endpoints for the embryos that were removed prior to blastocyst formation, we compared the AdaBoost prediction model (70% accuracy) with both the scDNA-seq data and observations collected from TLM. While 6 out of 16 (37.5%) of the embryos were predicted to develop to the blastocyst stage, when the scDNA-seq data was incorporated, only 4 of the 6 embryos (embryos 2, 5, 7 and 11) were predicted by AdaBoost algorithm to reach the blastocyst stage. However, all of these embryos were completely aneuploid. On the other hand, 5 of the 6 embryos (embryos 6, 12, 13, 14 and 16) which contained at least 1 euploid cell were predicted to fail. Besides CE, multipolar divisions and blastomere asymmetry were also annotated for all 16 embryos, but there was no association between the predicted outcome with blastomere symmetry or multipolar divisions between embryos containing aneuploid or euploid blastomeres ( $P>0.05$ ).

#### **Discussion:**

In our study, we used single cell sequencing to determine the exact ratio of euploid to aneuploid cells in the cleavage stage equine embryo and distinguished mis-segregation errors of meiotic and/or mitotic origin. In humans, aneuploidy rates of mitotic origin resulting in mosaicism have varied between 15%-90% [45]. This wide range is attributed to the various methods (aCGH, FISH, scDNA-seq), biopsy stage (cleavage stage, blastocyst stage) and the number of cells biopsied to assess ploidy status of an embryo [25,31,45,46]. Therefore, even though previous research have shown that the incidence of mitotic errors can be predicted based on the frequency of mosaic blastomeres present in a biopsied cleavage-stage embryo [45,47], the results are not consistent across studies [48,49].

Mosaic aneuploidy can affect pregnancy in humans, as lower clinical pregnancy outcomes have been associated with biopsied embryos with  $\geq 50\%$  mosaicism detected by the collection of 8-10 trophectoderm cells [18]. Furthermore, aneuploidy can manifest as uneven or asymmetrical blastomeres [47,50], and it has been shown that the incidences of aneuploidy can be propagated between the 2-cell stage and 4-cell stage resulting in lower implantation and pregnancy loss in humans 29.4% [47]. While our sample numbers were small, we also observed a much lower euploid to aneuploid ratio in embryos that were sequenced beyond the 4-cell stage. This could be due to the multipolar divisions, where embryos cleaved into 3 or as many as 5 cells during the first cleavage. Given the correlation between multipolar divisions and aneuploidy in other mammalian species [43,44,51], this may explain why we observed such a high percentage of aneuploid embryos and why embryo 15 was comprised entirely of blastomeres with chaotic aneuploidy.. Surprisingly, we observed that embryos which exhibited blastomere asymmetry were predicted to reach the blastocyst stage in TLM. However, because the dataset used to train the machine learning algorithm did not include embryo timepoints other than the mitotic events, we do not know if

blastomere asymmetry is truly associated with chromosomal abnormalities in the horse. It is also likely that morphological embryo grading such as blastomere symmetry can introduce variability in the data due to its subjectivity [52].

Sperm DNA fragmentation can also increase the rate of chromosomal abnormalities, specifically during the cleavage stage embryo [53,54] and this has been repeatedly shown (including by our lab) [55] that sperm exposed to high levels of oxygen free radicals can induce downstream adverse effects in embryos[55,56]. Furthermore, Daughtry and colleagues (2019) [31] have shown that a group of embryos with chaotic aneuploidy were linked to one particular sperm donor. In our study, we used sperm from a single donor for all ICSI sessions, and we do not know if sperm used for ICSI had low or high DNA fragmentation. However, due to our high percentage of aneuploid embryos, we predict that sperm with compromised DNA could have been a large factor in producing chaotic aneuploid embryos.

Besides being able to predict which embryos might successfully progress to the blastocyst stage [57], TLM has also been used to largely distinguish aneuploid and euploid embryos at multiple stages. In humans and bovine embryo studies, the onset of cleavage has been shown to be associated with aneuploidy [58,59]. Additionally, the duration of the first mitotic division and/or the time intervals between the second and third cleavage in aneuploid and mosaic embryos are more likely to deviate from cleavage times of euploid embryos [26,60]. However, it should be noted that these results are often biased because only blastocysts are biopsied, and any embryo that had become arrested are ignored.

Even though studies have claimed that aneuploidy can be predicted using TLM, our results disagree with these previous studies [58,59]. Because arrested embryos are not generally sequenced as mentioned above, this finding is puzzling, but is likely due to the small number of

embryos analyzed. If we had used methods other than scDNA-seq we may have mistakenly determined this embryo to be aneuploid. Similarly, blastocyst success was predicted in embryos that did not contain euploid blastomeres which is likely due to our 70% accuracy rate. Because our sequencing data included blastomeres with failed WGA, it is unknown if there could have been a euploid blastomere that was excluded from the analysis because of this limitation. There appears to be an added complexity for assessing aneuploid embryos in the horse, and embryos at a later cleavage stage should be sequenced to further investigate embryos that continue to develop and those that become arrested.

We are the first to report the percentage of aneuploid embryos using single-cell sequencing and establishing a prediction model using machine learning to assess blastocyst outcome in the horse. Our study reveals the high percentage of aneuploid cells during the early cleavage stage embryo. While our current prediction model only uses time-lapse data from our previous study, parameters such as CE, multipolar divisions and blastomere symmetry should be incorporated to improve predictions of embryos with higher percentage of euploid cells. A future application of this algorithm to TLM software will allow real-time embryo assessments to select the highest quality embryos for transfer.



## Tables and Figures

**Euploid, aneuploid and segmental blastomeres within equine embryos following ICSI**

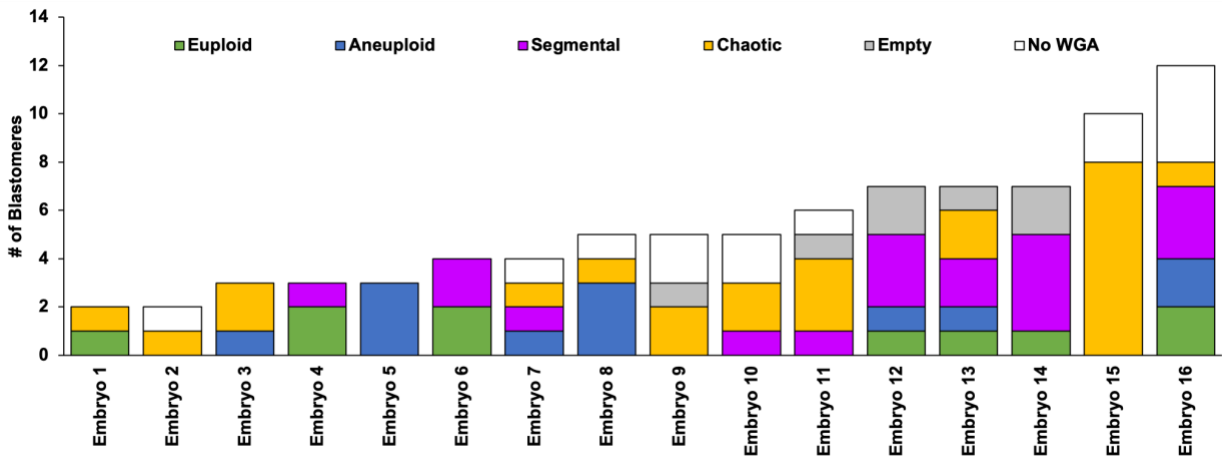


**Figure 4.1:** A summary of the chromosomal status in all blastomeres from embryos between 2-12 cell stages. Note that only 7 embryos contained at least one euploid blastomere. In contrast, most embryos consisted of at least 1 blastomere with chaotic aneuploidy, which is defined as having 5 or more chromosome losses and gains [31].

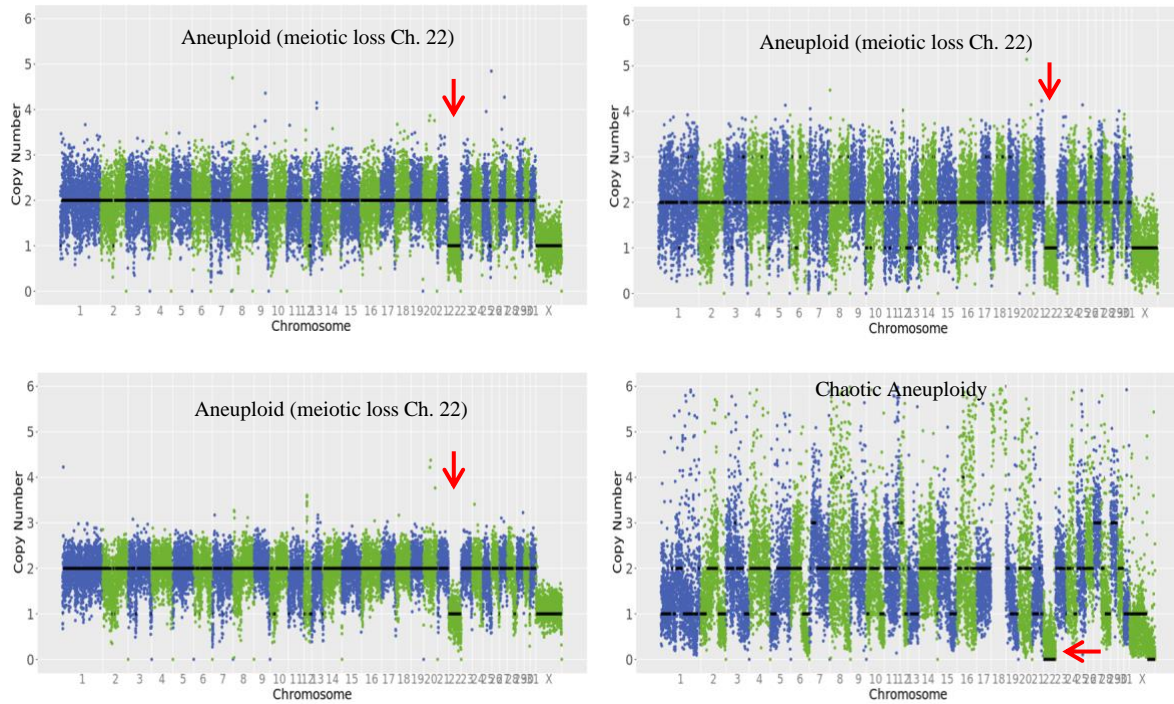


**Figure 4.2:** CNV analysis of individual blastomeres collected from embryo 5 showed the loss of 1-2 copies of chromosome 22. Reconstruction of the embryo revealed that the loss of chromosome 22 was the result of a meiotic error as only 1 copy is present in three of the blastomeres from this embryo. Chaotic aneuploidy, or the loss and/or gain of more than 4 chromosomes, was observed in the fourth blastomere, which also contained no copies of chromosome 22.

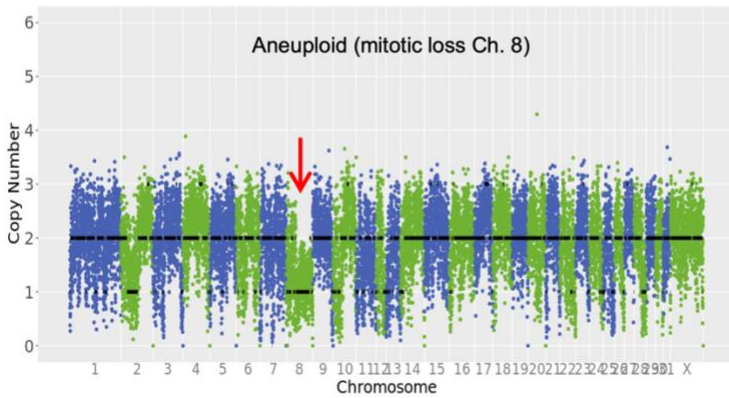
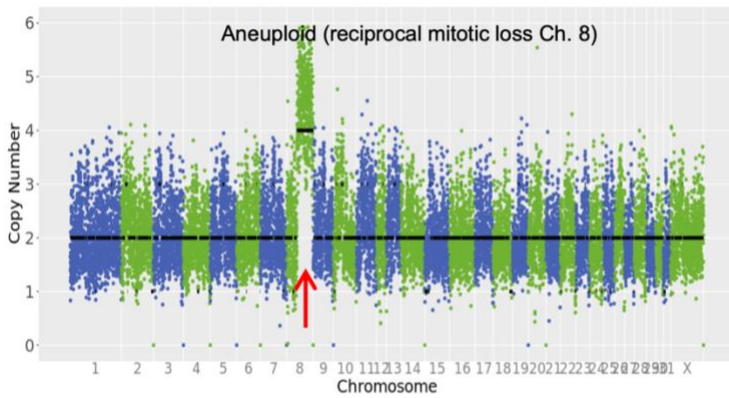
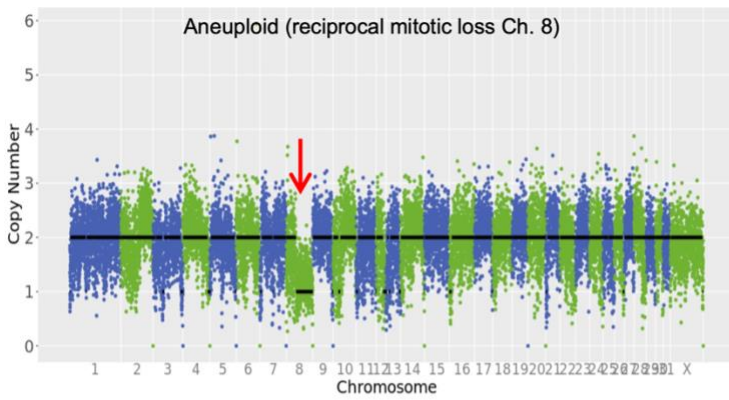


**Figure 4.3:** Chromosome plots showing a reciprocal mitotic loss and gain of chromosome 8 between blastomeres of embryo 9. This loss was also observed in a third blastomere from the embryo, which exhibited other whole and partial losses of different chromosomes.

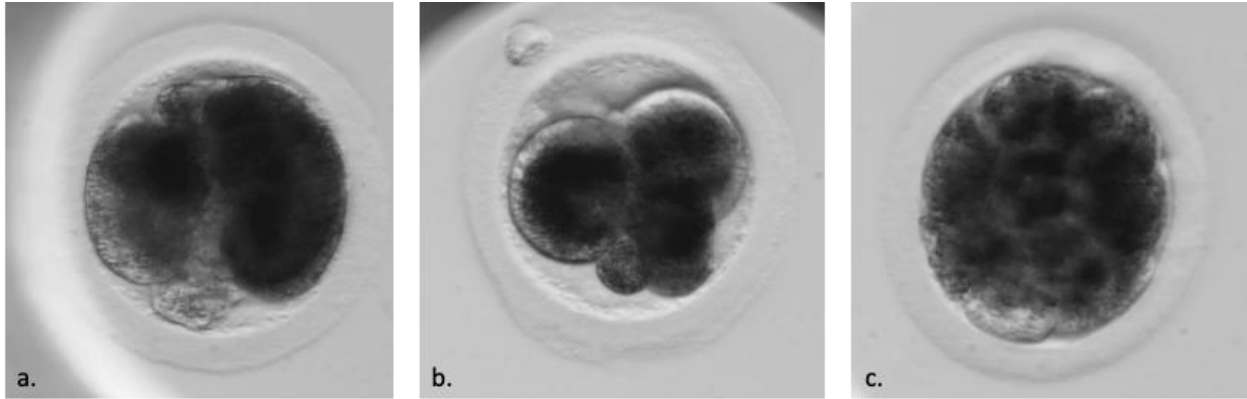


**Figure 4.4:** Multipolar divisions and blastomere asymmetry in early cleavage-stage equine embryos. Images were taken from the time-lapse videos from three different embryos (a.) blastomere asymmetry from a multipolar division at the zygote stage in embryo 7 (b.) a similar asymmetrical cleavage pattern was observed in embryo 5 (c.) Embryo 15 contained several cells that were produced from multiple multipolar divisions at 48 hrs post-ICSI. Based on our timeline established in equine[30], at this timepoint, the embryo should have only 4 blastomeres present. However, this embryo had at least 9 visible blastomeres.

**Table 4.1:** Comparison of predicted blastocyst results with time-lapse and single cell data

Embryo Number	Class probability	Predicted to reach blastocyst stage	Observations from time-lapse microscopy
1*	0.52	Yes	CE at zygote stage
2	0.56	Yes	CE at zygote stage; multipolar first division; 1:3 cells; blastomere asymmetry
3	0.48	No	CE at zygote stage; reverse cleavage at 3-cell stage
4*	0.56	Yes	CE at zygote stage; multipolar first division; 1:3 cells; blastomere asymmetry
5	0.58	Yes	CE; beautiful divisions; one cell may have been lost/lysed
6*	0.45	No	CE at zygote stage; multipolar first division; 1:5 cells; blastomere asymmetry; first division very late
7	0.53	Yes	CE, multipolar first division 1:3 cells, but reverse cleavage; 1st daughter cell then undergoes 1:3 cell division; blastomere asymmetry; cells may have been lost/lysed
8	0.48	No	CE at zygote stage; large fragments/small blastomeres; asymmetry if latter
9	0.37	No	CE, but large fragments
10	0.43	No	CE at zygote stage; cells may have been lost/lysed
11	0.52	Yes	CE, multipolar first division; 1:5 cells; partially arrested
12*	0.46	No	CE, but large fragments; cell may have been lost/lysed
13*	0.39	No	CE at zygote stage; multipolar first division; 1:5 cells
14*	0.42	No	CE at zygote stage; blastomeres divide on top of each other; cells may have been lost/lysed
15	0.33	No	CE at zygote stage; multipolar first division; 1:4 cells; cells may have been lost/lysed
16*	0.41	No	CE at zygote stage; multipolar first division; 1:4 cells

Class probability threshold was set to 0.5 where values  $>0.5$ =will reach blastocyst stage and values  $<0.5$ =will not reach blastocyst stage. \*denotes embryos with at least 1 euploid cell from the single-cell sequencing data (**Figure 1**). CE = cytoplasmic extrusion

## References

- [1] Yun Y, Wei Z, Hunter N. Maternal obesity enhances oocyte chromosome abnormalities associated with aging. *Chromosoma* 2019;128:413–21. doi:10.1007/s00412-019-00716-6.
- [2] Battaglia DE, Goodwin P, Klein NA, Soules MR. Fertilization and early embryology: Influence of maternal age on meiotic spindle assembly oocytes from naturally cycling women. *Hum Reprod* 1996;11:2217–22. doi:10.1093/oxfordjournals.humrep.a019080.
- [3] Rizzo M, Ducheyne KD, Deelen C, Beitsma M, Cristarella S, Quartuccio M, et al. Advanced mare age impairs the ability of in vitro-matured oocytes to correctly align chromosomes on the metaphase plate. *Equine Vet J* 2019;51:252–7. doi:10.1111/evj.12995.
- [4] Yun Y, Holt JE, Lane SIR, McLaughlin EA, Merriman JA, Jones KT. Reduced ability to recover from spindle disruption and loss of kinetochore spindle assembly checkpoint proteins in oocytes from aged mice. *Cell Cycle* 2014;13:1938–47. doi:10.4161/cc.28897.
- [5] Lagirand-Cantaloube J, Ciabrini C, Charrasse S, Ferrieres A, Castro A, Anahory T, et al. Loss of centromere cohesion in aneuploid human oocytes correlates with decreased kinetochore localization of the sac proteins Bub1 and Bubr1. *Sci Rep* 2017;7:44001. doi:10.1038/srep44001.
- [6] Pan H, Ma P, Zhu W, Schultz RM. Age-associated increase in aneuploidy and changes in gene expression in mouse eggs. *Dev Biol* 2008;316:397–407. doi:10.1016/j.ydbio.2008.01.048.
- [7] Tšuiiko O, Jatsenko T, Kumar L, Grace P, Kurg A, Vermeesch JR, et al. A speculative outlook on embryonic aneuploidy: Can molecular pathways be involved? 2019. doi:10.1016/j.ydbio.2018.01.014.
- [8] Jones KT, Lane SIR. Molecular causes of aneuploidy in mammalian eggs. *Development* 2013;140:3719–30. doi:10.1242/dev.090589.
- [9] Nabti I, Reis A, Levasseur M, Stemmann O, Jones KT. Securin and not CDK1/cyclin B1 regulates sister chromatid disjunction during meiosis II in mouse eggs. *Dev Biol* 2008;321:379–86. doi:10.1016/J.YDBIO.2008.06.036.
- [10] Cheng J-M, Li J, Tang J-X, Chen S-R, Deng S-L, Jin C, et al. Elevated intracellular pH appears in aged oocytes and causes oocyte aneuploidy associated with the loss of cohesion in mice. *Cell Cycle* 2016;15:2454–63. doi:10.1080/15384101.2016.1201255.
- [11] Munné S, Weier HUG, Grifo J, Cohen J. Chromosome Mosaicism in Human Embryos. *Biol Reprod* 1994;51:373–9. doi:10.1095/biolreprod51.3.373.
- [12] McCoy RC. Mosaicism in Preimplantation Human Embryos: When Chromosomal Abnormalities Are the Norm. *Trends Genet* 2017;33:448–63. doi:10.1016/j.tig.2017.04.001.
- [13] Ford E, Currie CE, Taylor DM, Erent M, Marston AL, Hartshorne GM, et al. The first mitotic division of the human embryo is highly error-prone. *BioRxiv* 2020:2020.07.17.208744. doi:10.1101/2020.07.17.208744.
- [14] Taylor TH, Gitlin SA, Patrick JL, Crain JL, Wilson JM, Griffin DK. The origin, mechanisms, incidence and clinical consequences of chromosomal mosaicism in humans n.d. doi:10.1093/humupd/dmu016.
- [15] Lane S, Kauppi L. Meiotic spindle assembly checkpoint and aneuploidy in males versus females. *Cell Mol Life Sci* 2019;76:1135–50. doi:10.1007/s00018-018-2986-6.

- [16] Shilton C, Kahler A, Davis B, Crabtree J, Crowhurst J, McGladdery A, et al. Whole genome analysis reveals aneuploidies in early pregnancy loss in the horse. *BioRxiv* 2020:2020.02.25.964239. doi:10.1101/2020.02.25.964239.
- [17] Cavazza T, Politi AZ, Aldag P, Baker C, Elder K, Blayney M, et al. Parental genome unification is highly erroneous in mammalian embryos. *BioRxiv* 2020:2020.08.27.269779. doi:10.1101/2020.08.27.269779.
- [18] Spinella F, Fiorentino F, Biricik A, Bono S, Ruberti A, Cotroneo E, et al. Extent of chromosomal mosaicism influences the clinical outcome of in vitro fertilization treatments. *Fertil Steril* 2018;109:77–83. doi:10.1016/j.fertnstert.2017.09.025.
- [19] Greco E, Minasi MG, Fiorentino F. Healthy Babies after Intrauterine Transfer of Mosaic Aneuploid Blastocysts. *N Engl J Med* 2015;373:2089–90. doi:10.1056/NEJMc1500421.
- [20] Fragouli E, Alfarawati S, Spath K, Babariya D, Tarozzi N, Borini A, et al. Analysis of implantation and ongoing pregnancy rates following the transfer of mosaic diploid-aneuploid blastocysts. *Hum Genet* 2017;136:805–19. doi:10.1007/s00439-017-1797-4.
- [21] Bolton H, Graham SJL, Van der Aa N, Kumar P, Theunis K, Fernandez Gallardo E, et al. Mouse model of chromosome mosaicism reveals lineage-specific depletion of aneuploid cells and normal developmental potential. *Nat Commun* 2016;7:11165. doi:10.1038/ncomms11165.
- [22] Carnevale EM. The mare model for follicular maturation and reproductive aging in the woman. *Theriogenology* 2008;69:23–30. doi:10.1016/j.theriogenology.2007.09.011.
- [23] Rizzo M, Preez N du, Ducheyne KD, Deelen C, Beitsma MM, Stout TAE, et al. The horse as a natural model to study reproductive aging-induced aneuploidy and weakened centromeric cohesion in oocytes. *Aging (Albany NY)* 2020;12:22220–32. doi:10.18632/aging.104159.
- [24] Munné S, Fragouli E, Colls P, Katz-Jaffe MG, Schoolcraft WB, Wells D. Improved detection of aneuploid blastocysts using a new 12-chromosome FISH test. *Reprod Biomed Online* 2010;20:92–7. doi:10.1016/j.rbmo.2009.10.015.
- [25] Starostik MR, Sosina OA, Mccoy RC. Single-cell analysis of human embryos reveals diverse patterns of aneuploidy and mosaicism 2020. doi:10.1101/gr.262774.120.
- [26] Chavez SL, Loewke KE, Han J, Moussavi F, Colls P, Munne S, et al. Dynamic blastomere behaviour reflects human embryo ploidy by the four-cell stage. *Nat Commun* 2012;3:1251. doi:10.1038/ncomms2249.
- [27] Hu DG, Webb G, Hussey N. Aneuploidy detection in single cells using DNA array-based comparative genomic hybridization. *Mol Hum Reprod* 2004;10:283–9. doi:10.1093/humrep/gah038.
- [28] Rambags BPB, Krijtenburg PJ, Van Drie HF, Lazzari G, Galli C, Pearson PL, et al. Numerical chromosomal abnormalities in equine embryos produced in vivo and in vitro. *Mol Reprod Dev* 2005;72:77–87. doi:10.1002/mrd.20302.
- [29] Foss R, Ortis H, Hinrichs K. Effect of potential oocyte transport protocols on blastocyst rates after intracytoplasmic sperm injection in the horse. *Equine Vet J* 2013;45:39–43. doi:10.1111/evj.12159.
- [30] Meyers S, Burrue V, Kato M, De La Fuente A, Orellana D, Renaudin C, et al. Equine non-invasive time-lapse imaging and blastocyst development. *Reprod Fertil Dev* 2019;31:1874–84. doi:10.1071/RD19260.
- [31] Daughtry BL, Rosenkrantz JL, Lazar NH, Fei SS, Redmayne N, Torkency KA, et al. Single-cell sequencing of primate preimplantation embryos reveals chromosome

- elimination via cellular fragmentation and blastomere exclusion. *Genome Res* 2019;29:367–82. doi:10.1101/gr.239830.118.
- [32] Krueger S, Giavalisco P, Krall L, Steinhauser M-C, Büssis D, Usadel B, et al. A Topological Map of the Compartmentalized *Arabidopsis thaliana* Leaf Metabolome. *PLoS One* 2011;6:e17806. doi:10.1371/journal.pone.0017806.
- [33] Chen C, Khaleel SS, Huang H, Wu CH. Software for pre-processing Illumina next-generation sequencing short read sequences. *Source Code Biol Med* 2014;9:8. doi:10.1186/1751-0473-9-8.
- [34] Kalbfleisch TS, Rice ES, DePriest MS, Walenz BP, Hestand MS, Vermeesch JR, et al. Improved reference genome for the domestic horse increases assembly contiguity and composition. *Commun Biol* 2018;1:197. doi:10.1038/s42003-018-0199-z.
- [35] Salavert Torres J, Blanquer Espert I, Domínguez AT, Hernández García V, Medina Castelló I, Tárraga Giménez J, et al. Using GPUs for the exact alignment of short-read genetic sequences by means of the Burrows-Wheeler transform. *IEEE/ACM Trans Comput Biol Bioinforma* 2012;9:1245–56. doi:10.1109/TCBB.2012.49.
- [36] Ramirez-Gonzalez RH, Bonnal R, Caccamo M, Maclean D. Bio-samtools: Ruby bindings for SAMtools, a library for accessing BAM files containing high-throughput sequence alignments. *Source Code Biol Med* 2012;7:6. doi:10.1186/1751-0473-7-6.
- [37] Vitak SA, Torkenczy KA, Rosenkrantz JL, Fields AJ, Christiansen L, Wong MH, et al. Sequencing thousands of single-cell genomes with combinatorial indexing. *Nat Methods* 2017;14:302–8. doi:10.1038/nmeth.4154.
- [38] Chen EY, Tan CM, Kou Y, Duan Q, Wang Z, Meirelles GV, et al. Enrichr: interactive and collaborative HTML5 gene list enrichment analysis tool. *BMC Bioinformatics* 2013;14:128. doi:10.1186/1471-2105-14-128.
- [39] B Z, SS H, X Z, R P, RR H, AE U. Whole-genome sequencing analysis of CNV using low-coverage and paired-end strategies is efficient and outperforms array-based CNV analysis. *J Med Genet* 2018;55. doi:10.1136/JMEDGENET-2018-105272.
- [40] AdaBoost. *Encycl. Biometrics*, Boston, MA: Springer US; 2009, p. 9–9. doi:10.1007/978-0-387-73003-5\_825.
- [41] Chavez SL, Loewke KE, Han J, Moussavi F, Colls P, Munne S, et al. Dynamic blastomere behaviour reflects human embryo ploidy by the four-cell stage. *Nat Commun* 2012;3. doi:10.1038/ncomms2249.
- [42] R. Core Team. *R: A language and environment for statistical computing* 2018.
- [43] McCoy RC, Newnham LJ, Ottolini CS, Hoffmann ER, Chatzimeletiou K, Cornejo OE, et al. Tripolar chromosome segregation drives the association between maternal genotype at variants spanning PLK4 and aneuploidy in human preimplantation embryos. *Hum Mol Genet* 2018;27:2573–85. doi:10.1093/hmg/ddy147.
- [44] Brooks KE, Daughtry BL, Davis B, Yan MY, Fei SS, Shepherd S, et al. Molecular contribution to embryonic aneuploidy and karyotypic complexity in initial cleavage divisions of mammalian development. *Development* 2022;149. doi:10.1242/dev.198341.
- [45] Mantikou E, Wong KM, Repping S, Mastenbroek S. Molecular origin of mitotic aneuploidies in preimplantation embryos. *Biochim Biophys Acta - Mol Basis Dis* 2012;1822:1921–30. doi:10.1016/J.BBADIS.2012.06.013.
- [46] van Echten-Arends J, Mastenbroek S, Sikkema-Raddatz B, Korevaar JC, Heineman MJ, van der Veen F, et al. Chromosomal mosaicism in human preimplantation embryos: a systematic review. *Hum Reprod Update* 2011;17:620–7. doi:10.1093/humupd/dmr014.



- [47] Hardarson T, Hanson C, Sjögren A, Lundin K. Human embryos with unevenly sized blastomeres have lower pregnancy and implantation rates: indications for aneuploidy and multinucleation. *Hum Reprod* 2001;16:313–8. doi:10.1093/humrep/16.2.313.
- [48] Mastenbroek S, Twisk M, van Echten-Arends J, Sikkema-Raddatz B, Korevaar JC, Verhoeve HR, et al. In Vitro Fertilization with Preimplantation Genetic Screening. *N Engl J Med* 2007;357:9–17. doi:10.1056/NEJMoa067744.
- [49] Baart EB, Martini E, van den Berg I, Macklon NS, Galjaard R-JH, Fauser BCJM, et al. Preimplantation genetic screening reveals a high incidence of aneuploidy and mosaicism in embryos from young women undergoing IVF. *Hum Reprod* 2006;21:223–33. doi:10.1093/humrep/dei291.
- [50] Shenoy CC, Khan Z, Coddington C, Jensen J, Daftary GS, Stewart EA, et al. Symmetry at the 4-cell stage using time-lapse imaging is correlated with embryo aneuploidy. *Fertil Steril* 2015;104:e309. doi:10.1016/j.fertnstert.2015.07.966.
- [51] Brooks KE, Daughtry BL, Metcalf E, Masterson K, Battaglia D, Gao L, et al. Assessing equine embryo developmental competency by time-lapse image analysis. *Reprod Fertil Dev* 2019;31:1840–50. doi:10.1071/RD19254.
- [52] Fernandez Gallardo E, Spiessens C, D’Hooghe T, Debrock S. Effect of embryo morphology and morphometrics on implantation of vitrified day 3 embryos after warming: a retrospective cohort study. *Reprod Biol Endocrinol* 2016;14:40. doi:10.1186/s12958-016-0175-8.
- [53] Middelkamp S, Van Tol HTA, Spierings DCJ, Boymans S, Guryev V, Roelen BAJ, et al. Sperm DNA damage causes genomic instability in early embryonic development. *Sci Adv* 2020;6:1–12. doi:10.1126/sciadv.aaz7602.
- [54] Burrueel V, Klooster K, Barker CM, Pera RR, Meyers S. Abnormal Early Cleavage Events Predict Early Embryo Demise: Sperm Oxidative Stress and Early Abnormal Cleavage. *Sci Rep* 2015;4:6598. doi:10.1038/srep06598.
- [55] Burrueel V, Klooster KL, Chitwood J, Ross PJ, Meyers SA. Oxidative damage to rhesus macaque spermatozoa results in mitotic arrest and transcript abundance changes in early embryos. *Biol Reprod* 2013;89. doi:10.1095/biolreprod.113.110981.
- [56] Lane SIR, Jones KT. Non-canonical function of spindle assembly checkpoint proteins after APC activation reduces aneuploidy in mouse oocytes. *Nat Commun* 2014;5:3444. doi:10.1038/ncomms4444.
- [57] Wong CC, Loewke KE, Bossert NL, Behr B, De Jonge CJ, Baer TM, et al. Non-invasive imaging of human embryos before embryonic genome activation predicts development to the blastocyst stage. *Nat Biotechnol* 2010;28:1115–21. doi:10.1038/nbt.1686.
- [58] Capalbo A, Hoffmann ER, Cimadomo D, Ubaldi FM, Rienzi L. Human female meiosis revised: New insights into the mechanisms of chromosome segregation and aneuploidies from advanced genomics and time-lapse imaging. *Hum Reprod Update* 2017;23:706–22. doi:10.1093/humupd/dmx026.
- [59] Hornak M, Kubicek D, Broz P, Hulinska P, Hanzalova K, Griffin D, et al. Aneuploidy Detection and mtDNA Quantification in Bovine Embryos with Different Cleavage Onset Using a Next-Generation Sequencing-Based Protocol. *Cytogenet Genome Res* 2017;150:60–7. doi:10.1159/000452923.
- [60] Vera-Rodriguez M, Chavez SL, Rubio C, Reijo Pera RA, Simon C. Prediction model for aneuploidy in early human embryo development revealed by single-cell analysis. *Nat Commun* 2015;6:7601. doi:10.1038/ncomms8601.

# Chapter 5

## Summary and Conclusions

In Chapter 1, I presented relevant information describing the gap in knowledge regarding embryonic development that exists in early equine embryo development comparative to other non-equid mammals. The experiments designed and conducted in Chapter 3 and 4 shed light on embryo morphokinetics and aneuploidy that may affect successful embryo development.

In Chapter 3, I used fluorescence microscopy and TLM to determine the pre-mitotic and mitotic events leading to the first cleavage. I have found that PN apposition and fusion occurs between 12 and 18 hrs in the horse. PN fusion is then followed by CE, which at this time, the parental genomes have unified based on fluorescence microscopy and the embryo is at metaphase of mitosis confirming that CE is a mitosis-related event in the horse. When the timing of CE in the successful blastocysts were compared to that of failed blastocysts, my data was consistent with previous findings in that earlier CE times were associated with blastocyst success. CE is a critical event in equine embryo development as PN apposition and fusion must complete for CE to occur, and it is a visual confirmation of successful fertilization as a mitotic event. We also determined that DNA is not contained within the granular material of CE, but only a few (n=3) embryos were analyzed by fluorescence and this warrants further investigation with a larger number of embryos and using a high-resolution approach such as next generation sequencing.

In Chapter 4, the percentage of aneuploid embryos was determined using single-cell sequencing for the first time in the horse. While embryos were removed between days 2 and 3 of embryo culture post ICSI, predictions using machine learning was used to determine if the embryos would have reached blastocyst stage or failed to reach blastocyst stage. Even though previous

studies have found an association between cleavage times and aneuploidy, our results did not reveal any association between the two. As these studies [1–5] evaluated hundreds of human embryos, it may also be due to the limited number of equine embryos that we analyzed here.

Future experiments investigating the exact contents of CE are necessary to fully understand its function during equine prometaphase and metaphase events. The embryos produced from the experiments were not transferred to assess pregnancy outcome, therefore, the significance observed in the timing of CE between successful and failed blastocyst groups should be further tested. Finally, parameters such as CE, multipolar divisions and blastomere symmetry should be incorporated in assessing equine embryos to improve predictions of embryos with higher percentage of euploid cells using machine learning technology. A future application of this algorithm to TLM software will allow real-time embryo assessments to select the highest quality embryos for transfer.

## References

- [1] Mantikou E, Wong KM, Repping S, Mastenbroek S. Molecular origin of mitotic aneuploidies in preimplantation embryos. *Biochim Biophys Acta - Mol Basis Dis* 2012;1822:1921–30. doi:10.1016/J.BBADIS.2012.06.013.
- [2] van Echten-Arends J, Mastenbroek S, Sikkema-Raddatz B, Korevaar JC, Heineman MJ, van der Veen F, et al. Chromosomal mosaicism in human preimplantation embryos: a systematic review. *Hum Reprod Update* 2011;17:620–7. doi:10.1093/humupd/dmr014.
- [3] Starostik MR, Sosina OA, Mccoy RC. Single-cell analysis of human embryos reveals diverse patterns of aneuploidy and mosaicism 2020. doi:10.1101/gr.262774.120.
- [4] Daughtry BL, Rosenkrantz JL, Lazar NH, Fei SS, Redmayne N, Torkency KA, et al. Single-cell sequencing of primate preimplantation embryos reveals chromosome elimination via cellular fragmentation and blastomere exclusion. *Genome Res* 2019;29:367–82. doi:10.1101/gr.239830.118.
- [5] Chavez SL, Loewke KE, Han J, Moussavi F, Colls P, Munne S, et al. Dynamic blastomere behaviour reflects human embryo ploidy by the four-cell stage. *Nat Commun* 2012;3. doi:10.1038/ncomms2249.